UNIVERSIDAD DE CÓRDOBA

INSTITUTO DE ESTUDIOS DE POSTGRADO

MÁSTER EN BIOTECNOLOGÍA

Trabajo Fin de Máster

BN-PAGE and LC-MS/MS proteomic techniques applied to the degradation of cyanide in *Pseudomonas pseudoalcaligenes* CECT5344

Miguel Ángel Aparicio Jiménez
Departamento de Bioquímica y Biología Molecular

María Dolores Roldán Ruiz
Directora del Trabajo

Víctor Manuel Luque Almagro
Codirector del Trabajo

Córdoba, 12/2016

María Dolores Roldán Ruiz (Universidad de Córdoba), Tutora y Directora del Trabajo y Víctor Manuel Luque Almagro (Universidad de Córdoba) Codirector del trabajo titulado "BN-PAGE and LC-MS/MS proteomic techniques applied to the degradation of cyanide in *Pseudomonas pseudoalcaligenes* CECT5344" realizado por Miguel Ángel Aparicio Jiménez, proponen como revisores de dicho trabajo a los Doctores:

- María de los Ángeles Alonso Moraga
- Gregorio Gálvez Valdivieso
- Ángel Llamas Azúa

Córdoba, diciembre 2016

Fdo. María Dolores Roldán Ruiz

Fdo. Víctor Luque Almagro

Index

Illustration Index

Illustration Index. Supplementary Material

Table Index

Table Index. Supplementary Material

1. Abstract

The cyanide-containing wastewaters from the jewellery industry constitute a serious problem of pollution. The use of cyanotrophic microorganisms is currently proposed as a successful alternative to physico-chemical methods to remove cyanide from polluted areas. *Pseudomonas pseudoalcaligenes* CECT5344 is a bacterium with a great potential in removing cyanide from the environment, because this strain is able to assimilate cyanide and cyano-derivatives under alkaline conditions. In this work, the BN-PAGE (Blue Native-Polyacrylamide Gel Electrophoresis) technique has been applied to identify proteins complexes induced by cyanide. The results reveal the presence of two possible complexes; complex I that is composed of a phosphoenolpyruvate synthase and DnaK chaperone, and complex II formed by the pyruvate carboxylase and the phosphoenolpyruvate carboxylase. These proteins function to specifically produce oxaloacetate in response to cyanide. Oxaloacetate reacts with cyanide to produce a nitrile, which is converted to its respective carboxylic acid and ammonium by the nitrilase NitC, encoded by the *P. pseudoalcaligenes* CECT5344 *nit1C* gene cluster. NitA is a positive transcriptional regulator that responds to cyanide. In addition, a biochemical characterization of the *nitA*$^-$ and *nitC*$^-$ mutants of *P. pseudoalcaligenes* CECT5344 that are unable to assimilate cyanide has been carried out by analyzing their proteome in response to cyanide. Comparative experimental designs were carried by using the Progenesis IQ software. Thus, the proteomes of all three strains were compared in pairs, *nitA*$^-$ *versus* wild-type, *nitC*$^-$ *versus* wild-type and *nitA*$^-$ *versus nitC*$^-$. The mutant strain *nitA*$^-$ showed induced proteins related to protection against exogenous DNA and general oxidative stress, polyhydroxyalakanoate metabolism and amino acids metabolism, while repressed proteins were related to the Nit1C system, carbon metabolism, metal extrusion system and terminal electron acceptor in respiration. The mutant strain *nitC*$^-$ displayed induced proteins related to nitrogen starvation and general oxidative stress response, while repressed proteins were related to the Nit system, carbon metabolism, metal extrusion system and terminal electron acceptor in respiration.

2. Objectives

The main objectives of this work have been:

1. Identification of protein complexes induced by cyanide in *P. pseudoalcaligenes* CECT5344.
2. Physiological and proteomic characterization of the *nitA*$^{-}$ and *nitC*$^{-}$ mutants of *P. pseudoalcaligenes* CECT5344 strain affected in cyanide assimilation.

3. Introduction

3.1. The chemistry of cyanide

Cyanide is a triple-bonded molecule formed by carbon and nitrogen that can be found in the protonated form, as hydrogen cyanide (HCN), or as anion (CN^-). Other chemical forms adopted by this compound are cyanide salts (NaCN or KCN), metal-cyanide chemical complexes and nitriles, also called organic cyanides (Blumer and Haas 2000; Kuyucak and Akcil, 2013; Mirizadeh *et al.,* 2014).

Cyanide is one of the most toxic chemicals for living beings (Li *et al*., 2011). Despite of cyanide toxicity, it has been proposed in many studies that cyanide has played a key role in the origin of life because in a solution with HCN and ammonium, adenine was produced by polymerization of five molecules of HCN (Matthews and Minard, 2006; Sutherland, 2016).

3.2. Cyanide toxicity

The molecular mechanism by which cyanide exerts its toxicity is based on the high affinity of this compound for metals, inhibiting metalloenzymes like the iron/copper-containing terminal oxidase of the respiratory chain (cytochrome *c* oxidase). The inhibition of the respiratory chain leads to the inhibition of ATP synthesis. Furthermore, sublethal doses of cyanide produce a sharp decrease in the rate of glycolysis and a complete inhibition of the Krebs cycle (Xu *et al.,* 2010).

3.3. Sources of cyanide

3.3.1. Anthropogenic sources

Cyanide is a chemical compound worldwide used in many industrial processes, mainly in industries related to the manufacture of metals like mining, electroplating and steel manufacture. Because of the extended use of cyanide, this compound is frequently

present in wastewaters generated by a large number of industries like petrochemistry, photographic, and nitriles, acrylic plastics and rubber production (Xu *et al.,* 2010). The cyanide used in some of these synthetic processes represents about 80% of the total cyanide produced worldwide each year (Fig. 1), while 18% cyanide is consumed for mining (Logsdon *et al.,* 1999). Cyanide-containing residues are spilled into nature, causing the death of the wildlife (Boening and Chew, 1999; Dash *et al.,* 2009).

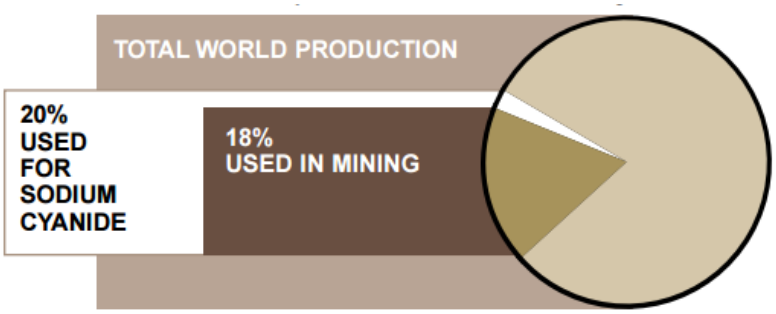

Figure 1. Worldwide production of cyanide. The largest portion refers to cyanide utilized in production of organic chemicals (80%). 20% remained corresponds to cyanide used for sodium cyanide production, which is mainly consumed for mining, 18% of the whole, (Logsdon *et al.,* 1999).

Regarding the utilization of cyanide in gold mining, Acheampong and collaborators (2010) described in detail the extraction of gold from ores using alkaline cyanidation. This process begins with the crushing of the ore, approximately to 100 microns. Then, the gold is sent to a leaching plant where lime, cyanide and oxygen are added. The lime produces an increase of the pH, while oxygen and cyanide react with gold by the reaction of cyanidation, as follows:

$$4\ Au + 8\ NaCN + O_2 + 2\ H_2O \rightarrow 4\ Na[Au(CN)_2] + 4\ NaOH$$

This cyanide solution allows the release of gold from the ore. Finally, this solution is collected and gold is precipitated.

The main producers of gold are China, Australia, Russia, the United States of America and Africa. Furthermore, in Europe, the mining activities are currently becoming more popular because of the high demand of gold for the jewelry industry (Luque-Almagro *et al.,* 2016)

3.3.2. Natural sources

Cyanide can be produced by a wide type of organisms that are called cyanogenics, as a product of their metabolism. Among these, some algae, fungi, plants, and even arthropods are found (Dash *et al.,* 2009). The ability to produce cyanide from a biological source was discovered in 1871 in fungi (Basidiomycetes belonging to the *Marasmius* genus), and latest in other organism but cyanogenesis in bacteria was first demonstrated in *Chromobacterium violaceum* strains (Michaels and Corpe, 1965).

Although cyanide is potentially dangerous, poisoning by bacterial cyanide has not been reported in eukaryotes, probably because cyanogenesis is strictly regulated in bacteria. Nevertheless, in massive infections of host cells by *Pseudomonas aeruginosa* the hazardous effect of cyanide could be significant (Blumer and Haas, 2000).

In plants, cyanide is produced during the synthesis of ethylene, and in some cases cyanide is also generated as a part of cyanogenic glycosides like the amygdalin. It is worth to mention that some fruits accumulate cyanide during some phases of their life cycle, such as apricots, bean sprouts, cashews, cherries, chestnuts, corn, potatoes, soybeans, walnuts, etc. The biological role of cyanogenesis is related to defense against herbivores or pathogens (Logsdon *et al.,* 1999; Blumer and Haas 2000; Xu *et al.,* 2010).

3.4. Biodegradation of cyanide

To remove cyanide from industrial wastewaters, different physico-chemical methods have been developed. Among these, alkaline chlorination, sulfur oxide/air and hydrogen peroxide processes have been described. Nevertheless, these techniques are very expensive and dangerous because the compounds used or the by-products generated, constitute also a source of pollution. The use of cyanotrophic microorganisms able to degradate or assimilate cyanide has been proposed as a good alternative to the physico-chemical methods. For cyanide biodegradation, the pK_a of cyanhidric acid (9.2) is a relevant factor to be considered. Thus, pH values higher than 9.2 have to be established

during the degradation process to avoid the conversion of the soluble anion cyanide into the volatile hydrogen cyanide (Mirizadeh *et al.,* 2014; Luque-Almagro *et al.,* 2015).
Several cyanide assimilation pathways have been described in different cyanotrophic microorganisms. These pathways include hydrolytic, oxidative, reductive and substitution/transfer reactions (Fig. 2), besides of a thiocyanate degradation route (Ebbs, 2004).

In the hydrolytic pathways, cyanide is converted into formate and ammonia by the cyanidase or into formamide by the action of the cyanide hydratase, which is mainly produced by fungi, and is extremely conserved within species. On the other hand, cyanidase is mainly produced by bacteria. Nitrilases and nitrile hydratases catalyze the hydrolysis of organic cyanides (nitriles) to ammonia and the corresponding carboxylic acid. These enzymes exhibit lower substrate specificity than cyanidases or cyanide hidratases.
The cyanide dioxygenase catalyzes the oxidation of cyanide to ammonia and carbon dioxide. Regarding to the reductive pathway, nitrogenase can use cyanide as substrate forming different products, depending on the number of electrons that are transferred to the substrate, two, four or six, to produce CH_2NH, CH_3NH_2 or CH_4 and NH_3, respectively (Raybuck, 1992).

The substitution/transfer reactions are catalyzed by the 3-cyanoalanine synthase that can use either cysteine or *O*-acetylserine in combination with CN. Thiocyanate is produced *in vivo* by a wide variety of microorganisms through the substitution/transfer mechanism carried out by a cyanide sulfurtransferase. Some bacterial strains are able to degradate this compound by the sequential action of two enzymes, the thiocyanate hydrolase that catalyzes the conversion of thiocyanate into cyanate and the cyanase that converts cyanate into carbon dioxide and ammonium.

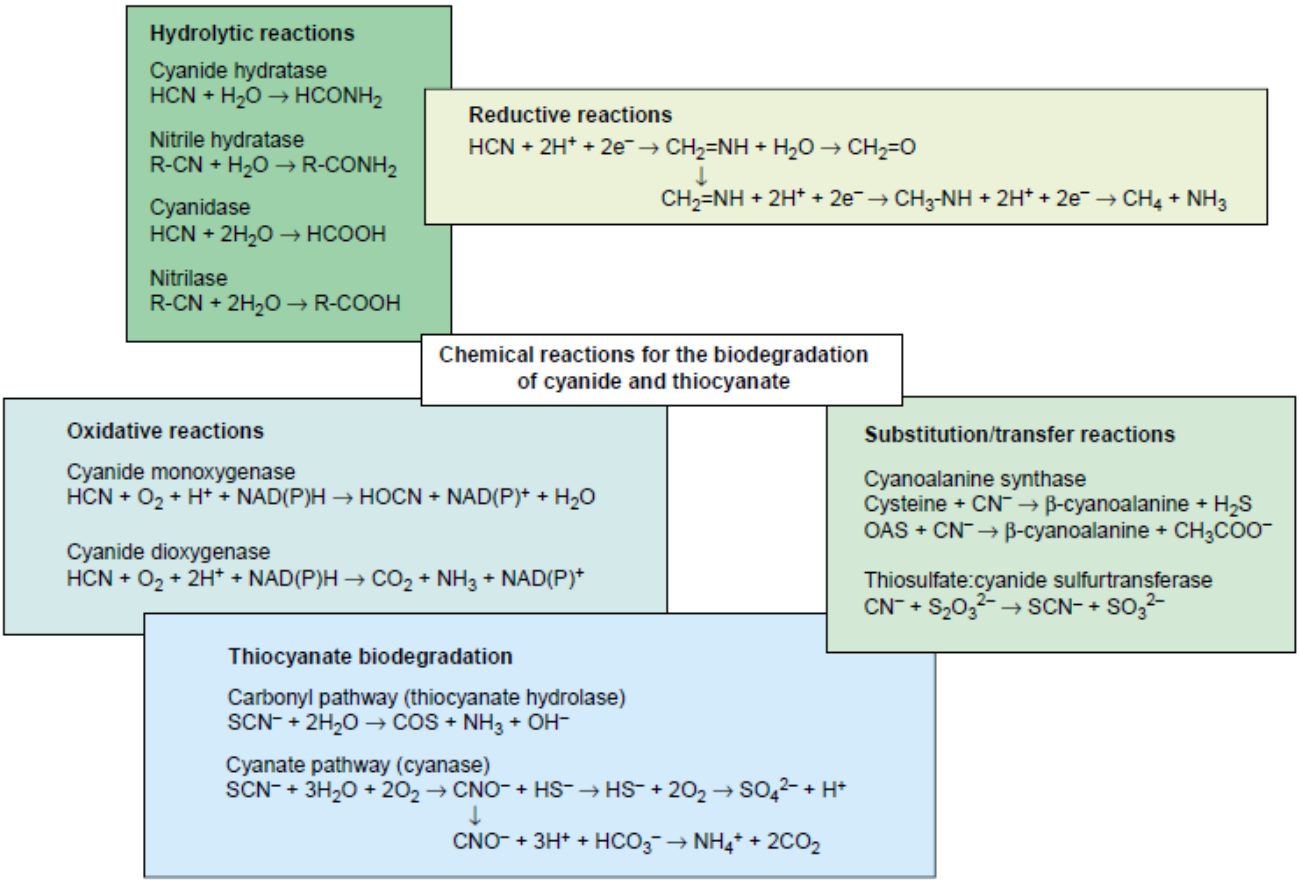

Figure2. Cyanide and thiocyanate assimilation pathways. Among these, hydrolytic, reductive, oxidative, substitution/transfer reactions have been described. The degradation pathways for thiocyanate are also shown (Ebbs, 2004**).**

3.5. The cyanotrophic bacterium *Pseudomonas pseudoalcaligenes* CECT5344

Pseudomonas pseudoalcaligenes CECT5344 is one of the most widely studied cyanotrophic bacteria. This bacterial strain, isolated from the Guadalquivir River (Córdoba, Spain) displays a great potential for cyanide biodegradation because it is an alkalophilic bacterium. The pK_a of HCN is 9.2, thus, the utilization of alkaline growth medium allows cyanide to be retained in the media as soluble form (CN^-), avoiding the formation of the HCN gas. In addition to cyanide, the strain CECT5344 is also able to assimilate cyano-derivatives such as cyanate, 3-cyanoalanine, cyanacetamide and nitroferricyanide, as well as metal-cyanide complexes present in wastewaters from the jewelry industry (Luque-Almagro *et al.,* 2005).

The cyanide assimilation pathway of *P. pseudoalcaligenes* CECT5344 involves formation of nitrile of oxaloacetate formation as intermediate (Fig. 3). To accomplish this process, this strain has a malate quinone:oxidoreductase (MqoA) that generates oxaloacetate, which reacts chemically with cyanide to produce a 2-hydroxynitrile. This compound is converted into ammonium and the corresponding carboxylic acid by the nitrilase NitC. (Luque-Almagro *et al.,* 2011; Estepa *et al.,* 2012). Besides, this bacterium has a cyanide insensitive cytochrome oxidase system (CioAB) to avoid the inhibition of the respiratory chain caused by the binding of cyanide to the aa_3-type terminal oxidase (Quesada *et al.,* 2007).

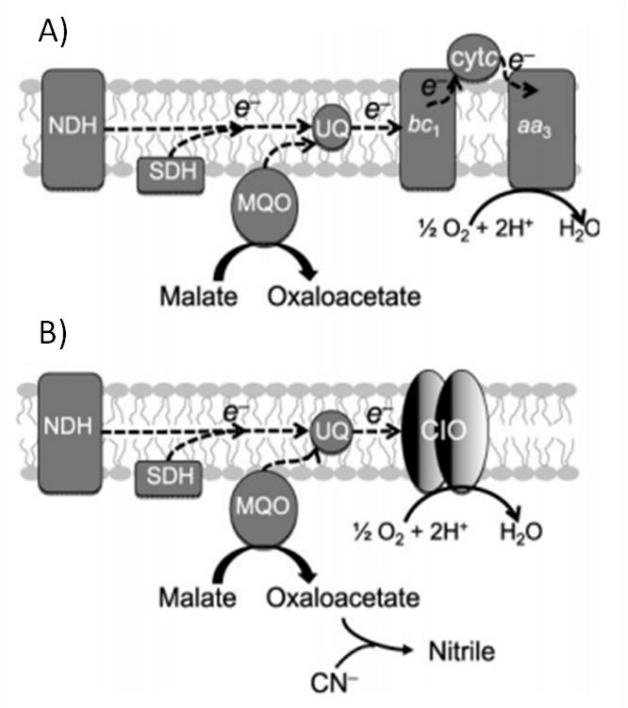

Figure 3. Respiratory electron transport chain in *P. pseudoalcaligenes* CECT5344. (A) Non-cyanotrophic conditions. (B) Cyanotrophic conditions (Luque-Almagro *et al.,* 2011).

The nitrilase NitC involved in cyanide assimilation is encoded by the *nitC* gene, which belongs to the *nit1C* gene cluster (Fig. 4). Excluding NitA and NitC proteins, most of the proteins encoded by the *P. pseudoalcaligenes* CECT5344 *nit1C* gene cluster have unknown function. The *nit1C* cluster presents a length of 7.8 kb, and includes eight genes (Estepa *et al*., 2012). In addition to the *nitC* gene, the genome of *P. pseudoalcaligenes*

CECT544 contains other three genes coding for putative nitrilases (Luque-Almagro *et al.*, 2013).The putative nitrilases are non-essential for cyanide assimilation in the strain CECT5344, but may play a role in cyanide detoxification, because they have been found induced by cyanide in transcriptomic studies (Luque-Almagro *et al.,* 2015).

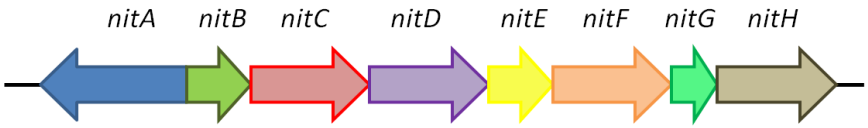

Figure 4. ***P. pseudoalcaligenes*** **CECT5344** ***nit1C*** **gene cluster.** This gene cluster contains the following genes: *nitA,* transcriptional activator; *nitB* and *nitG* unknown function; *nitC*, nitrilase; *nitD,* member of the *S*-adenosylmethionine superfamily; *nitE,* member of the *N*-acyltransferase superfamily; *nitF,* involved in *de novo* purine synthesis; *nitH,* NADPH-dependent flavin oxidoreductase.

The whole genome sequence of the CECT5344 strain has been completely sequenced (Luque-Almagro *et al.,* 2013; Wibberg *et al.,* 2014; Wibberg *et al.,* 2016). *P. pseudoalcaligenes* CECT5344 is the first cyanotrophic microorganism whose transcriptome has been studied in response to cyanide by using DNA microarrays (Luque-Almagro *et al.,* 2015). In addition, there are previous proteomic studies by using global analysis techniques such as LC-MS/MS to analyze the response of the CECT5344 strain to cyanide (Ibañez *et al.,* unpublished)

Liquid chromatography coupled with mass spectrometry is very useful to quantify and identify peptides in complex biological samples. The protein abundance of a sample is measured by digesting the proteins with tripsin to produce peptides that are separated by LC (Liquid Chromatography), ionized and finally analyzed by Mass Spectrometry (Matzke *et al.,* 2013).

BN-PAGE (Blue Native Polyacrylamide Gel Electrophoresis) is a technique designed for the separation of cellular protein complexes. This technique consist of two dimensions,

the first is performed under native conditions to separate the proteins according to their shape, length and molecular weight, and the second is carried out under denaturing conditions to separate the subunits from the protein complexes (Reisinger and Eichacker, 2008).

4. Materials and Methods

4.1. Biological material and culture conditions

The wild-type strain and the *nitA*$^-$ and *nitC*$^-$ mutant strains of *P. pseudoalcaligenes* CECT5344 were used in this work. The bacterial strains were cultured in minimal liquid medium M9 (Maniatis *et al.,* 1982) which present the following composition (per liter):

Na_2HPO_4…….. 6 g

KH_2PO_4……. 3 g

NaCl…… 0.5 g

Sodium acetate…… 4.1 g

Trace metals solution…… 1.25 ml

The pH of the media was adjusted to 9.5 and the nitrogen source used was ammonium chloride or sodium cyanide at the indicated concentrations for each experiment.

The trace metals solution was prepared with the following chemical compounds (per liter): 10.75 g $MgCl_2$, 2 g $CaCO_3$, 6.16 g $MgSO_4$ x $7H_2O$, 4.75 g $FeSO_4$ x $7H_2O$, 1.44 g $ZnSO_4$ x $7H_2O$, 1.12 g $MnSO_4$ x $7H_2O$, 0.25 g $CuSO_4$ x $5H_2O$, 0.28 g $CoSO_4$ x $7H_2O$, 0.06 g H_3BO_3 and 51.13 ml 12 N HCl.

The bacterial strains were cultured under aerobic conditions at 30 ^oC at 240 rpm into an orbital shaker. Cultures were harvested by centrifugation at 20 000 *g* during 10 minutes and 4 ^oC. The supernatant was discarded and cells were washed with 50 mM Tris-HCl (pH 8) buffer. Finally, cell pellets were stored at -80 ^oC until use.

4.2. Analytical assays

4.2.1. Measurement of bacterial growth

The bacterial growth was monitored by measuring the absorbance of the culture at 600 nm (A_{600nm}) or measuring the total protein concentration in whole cells by the Lowry method described below (Shakir *et al.,* 1994)

4.2.2. Determination of ammonium concentration

The concentration of ammonium was measured by using the Nessler method (Morrison, 1971). According to this method, 0.5 ml Nessler reagent (1:1 mixture solution A with 0.09 M K_2HgI_4 and solution B with 2.5 M KOH) were added to 0.5 ml of sample. After 5 minutes of incubation at room temperature, the absorbance at 410 nm was measured.

An additional method to determine ammonium concentration described by Solorzano (1969) was also used. To carry out this method, the following reagents were prepared:

- Reagent A: phenol-alcohol solution. 1.5 ml phenol mixed with 15 ml ethanol.
- Reagent B: 0.5% (w/v) sodium nitroprusside.
- Reagent C: 20% (w/v) trisodium citrate and 1% (w/v) sodium hydroxide.
- Reagent D: 12.5% (w/v) sodium hypochlorite solution.
- Reagent E: This mixture was prepared immediately before its use with 20 ml reagent C and 5 ml reagent D.

The method was carried out by diluting 100 µl of sample in 2.7 ml of deionized water and 0.2 ml reagent A and 0.2 ml reagent B were added. Finally, 0.5 ml reagent E was added, and after one hour and a half of incubation at room temperature, the absorbance of the solution was measured at 640 nm.

For each method, the concentration of ammonium was estimated by using a calibration plot previously elaborated with ammonium chloride.

4.2.3. Determination of cyanide concentration

The concentration of cyanide was determined according to Asmus and Garschagen (1953). In this method, 100 µl of chloramine T 1% (w/v) were added to 2.5 ml of sample. After 1 minute, 300 µl of a reagent containing 3 g barbituric acid, 15 ml pyridine, 3 ml HCl and 29 ml of water were added. This mixture was incubated during 5 minutes at room temperature and the absorbance was monitored at 578 nm.

The concentration of cyanide was estimated by using a calibration plot previously elaborated with sodium cyanide.

4.2.4. Determination of protein concentration

Two different methods were used to determine protein concentration.

The Bradford method (Bradford, 1976) was used to determine protein concentration in crude extracts and was carried out using 800 µl of sample and 200 µl of Bradford reagent (BIORAD). After 5 minutes of incubation at room temperature, the absorbance at 595 nm was measured. The absorbance data were transformed to concentration by using a calibration plot performed with bovine serum albumin.

A modified Lowry method (Shakir *et al.* 1994) was used to determine protein concentration in whole cells, and four reagents were prepared:

- Reagent A: 4% (w/v) CO_3Na_2 and 0.2 N NaOH.
- Reagent B: 2% (w/v) SO_4Cu x $5H_2O$.
- Reagent C: 4% (w/v) Sodium and potassium tartrate.
- Reagent D: 10 ml reagent A + 10 ml H_2O + 0.1 ml reagent C + 0.1 ml reagent B.

Samples were obtained collecting 1 ml of the bacterial culture followed by a centrifugation at 10 000 *g* for five minutes. The cell pellet was resuspended in 1 ml of 50 mM Tris-HCl buffer (pH 8). 250 µl of the sample were mixed with reagent D. This mixture was incubated at room temperature for 10 minutes then at 37 ^oC for 3 minutes. Finally,

125 µl of Folin reagent diluted 1/2 (Folin Ciocalteu´s reagent, Panreac) were added and incubated at 37 ºC for 3 minutes. The absorbance at 750 nm was measured and the concentration of protein was determined by using a calibration plot carried out with a solution of bovine serum albumin.

4.3. Nitrilase activity assay

The nitrilase activity was assayed in whole cells grown in minimal M9 media with 2 mM NH_4Cl or 2 mM NaCN as nitrogen source. Cells were harvested by centrifugation at 20 000 *g* and 4 ºC for 10 minutes. Cell pellets were resuspended in 100 mM sodium phosphate buffer (pH 7) and concentrated until an A_{600nm} of about 1.7. This cellular suspension (1 ml) was incubated with 100 mM glutaronitrile as substrate at 30 ºC for 30 minutes. Ammonium produced was determined according to the Solorzano method described above (Solorzano, 1969).

4.4. BN-PAGE (Blue Native Polyacrylamide Gel Electrophoresis)

In order to identify proteins complexes induced by cyanide, the BN-PAGE technique was applied in *P. pseudoalcaligenes* CECT5344 cells grown with cyanide or ammonium as nitrogen source. This method consists of a first dimension carried out under native conditions, followed by a second dimension under non-native conditions with SDS (sodium dodecyl sulfate) (Wittig *et al.,* 2006; Fiala *et al.,* 2011).

4.4.1. Preparation of polyacrylamide gels

In the first dimension, a 7-15% gradient polyacrylamide gels (8.6 x 7.2 cm and 1 mm of thickness) were used (Table 1).

The polymerization of gels was performed by using the Mini-PROTEAN 3 Multi-Casting Chamber (BioRad) and the Gradient Former 30-100 ml Model 385 (BioRad). On the other hand, the gels used for the second dimension have a size of 16 x 20 cm, 1.5 mm of thickness. Polyacrylamide gels for the second dimension were prepared as specified in Table 2.

Table 1. Composition of native polyacrylamide gels. *3X BN buffer composition: 75 mM imidazole and 200 mM ε-aminocaproic acid (pH 7).

	7% solution	**15% solution**
30% Acrylamide/Bis Solution (BioRad)	7% (1.04 ml)	15% (2.5 ml)
Deionized water	2.13 ml	-
Glicerol 70%	-	620 µl
3X BN buffer*	1.83 ml	1.83 ml
Ammonium persulfate 10%	18 µl	14 µl
TEMED	1.8 µl	1.4 µl

Table 2. Composition of denaturing polyacrylamide gels. *4X Lower buffer composition: 1.5 M Tris and 0.4% (w/v) SDS (pH 8.8). ** 4X Upper buffer composition: 0.5 M Tris and 0.4% (w/v) SDS (pH 6.8).

Resolving (10%)	
30% Acrylamide/Bis Solution (BioRad)	10% (13.3 ml)
Deionized water	18 ml
4X Lower buffer*	10 ml
Ammonium persulfate 10%	268 µl
TEMED	40 µl

Stacking (4.8%)	
30% Acrylamide/Bis Solution (BioRad)	4.8 % (800 µl)
Deionized water	2.9 ml
4X Upper buffer**	1.25 ml
Ammonium persulfate 10%	50 µl
TEMED	5 µl

4.4.2. Sample preparation

The soluble fractions loaded into the native polyacrylamide gels were obtained from *P. pseudoalcaligenes* CECT5344 cells cultured in M9 media with 2 mM ammonium or 2 mM cyanide as nitrogen source. Cells were harvested and resuspended in a buffer containing 50 mM imidazole, 2 mM 2-aminocaproic acid and 1 mM EDTA (pH 7). Cells were broken by cavitation (three pulses of five seconds each one at 90 W). Then they were centrifuged at 20 000 *g* to separate the membranes from the soluble fraction. After centrifugation, the supernatant was concentrated by using a centricon Amicon Ultra-0.5 ml (Millipore) to reach a protein concentration of approximately 10 µg/µl. About 200 µg were loaded into each well of the polyacrylamide gel.

4.4.3. Native electrophoresis

This electrophoresis was carried out using the Mini-PROTEAN® Tetra Vertical Electrophoresis Cell (BioRad).

Two different buffers were used: the cathode buffer was prepared avoiding the use of SDS. 0.002% (w/v) Coomassie Brilliant Blue G250 was added to supply a negative charge to the proteins. In addition, 7.5 mM imidazole and 50 mM Tricine were added to the buffer and the pH was adjusted to 7. The anode buffer was prepared with 25 mM imidazole and 50 mM Tricine.

After loading samples into the wells, an initial voltage of 100 V was applied until the samples entered into the gel, and then, the voltage was increased to 180 V. After electrophoresis, lanes were excised from the gel and they were incubated for 30 min with a reductive solution containing 1% (w/v) SDS and 1% β-mercaptoethanol.

4.4.4. Second dimension (SDS-PAGE)

Lanes from the native electrophoresis were placed over the top of a polyacrylamide denaturing gel. Two lanes were used per gel (one corresponding to proteins from cells grown with ammonia and another corresponding to proteins from cells grown with cyanide). Finally, 0.4% (w/v) agarose, was added to seal the lanes.

Initially the electrophoresis was performed at 15 mA/gel and after 15 minutes, the voltage was increased to 30 mA/gel.

After the electrophoresis was performed, gels were incubated for one hour in a fixing solution containing 7% acetic acid and 25% methanol. Staining was performed overnight by using Coomassie Blue G250 solution (Sigma-Aldrich) diluted 1/5 with methanol.

Gels were destined in a solution containing 10% acetic acid and 25% methanol, followed by incubation with a 25% methanol solution. After, gels were scanned and the spots that were aligned vertically identified, as possible part of the same complex by MALDI-TOF/TOF.

4.5. Proteomic analysis (LC-MS/MS)

4.5.1 Sample preparation

For this proteomic approach, wild-type strain and *nitA*$^{-}$ and *nitC*$^{-}$ mutant strains were grown with 2 mM cyanide. For each strain, three experimental replicates were prepared.

Cell pellets were resuspended using 500-800 µl of a buffer containing 8 M urea, 4% w/v CHAPS and 40 mM Tris-base buffer solution. To remove DNA from samples, DNAase were added.

Cells were broken by cavitation (three pulses of five seconds at 90 W) and centrifuged at 10 000 *g* and 4 ºC for 1.5 h. The pellet was discarded, and the protein content was determined in the supernatant.

Subsequently, proteins were precipitated by using 2D-Clean Up Kit (GE Healthcare) according to manufacturer's instructions. Finally, proteins were resuspended overnight in 150 µl 6 M urea solution at room temperature with gentle shaking.

Protein quantification was performed in the samples by using the Bradford method.

4.5.2. Treatment of samples

Samples were digested with trypsin overnight at 37 °C with top-down agitation. All analyses were performed with a Dionex Ultimate 3000 nano UHPLC system (Thermo Fisher Scientific, Waltham-MA, USA) connected to a mass spectrometer LTQ Orbitrap XL (Thermo Fisher Scientific, Waltham-MA, USA) equipped with nanoelectrospray ionization interface. The separation column was Acclaim Pepmap C18, 150 mm × 0.075 mm, 3 µm pore size (Thermo Fisher Scientific, Waltham-MA, USA). For trapping of the digest, it was used a 5 mm × 0.3 mm precolumn Acclaim Pepmap C18 (Agilent Technologies, Waldbronn, Germany). One fourth of the total sample volume, corresponding to 5 µl, was trapped at 10 µl/min flow rate, for 5 min, with 2% acetonitrile/0.05% trifluoroacetic acid. After that, the trapping column was switched on-line with the separation column and the gradient was started. Peptides were eluted with a 60-min gradient of 5–40% acetonitrile/0.1% formic acid solution at a 300 nl/min flow rate. MS data (Full Scan) were acquired in the positive ion mode over the 400–1500 m/z range. MS/MS data were acquired in dependent scan mode, selecting automatically the five most intense ions for fragmentation, with dynamic exclusion set to on. In all cases, a nESI spray voltage of 1.9 kV was used. Tandem mass spectra were extracted using Thermo Proteome Discoverer 2.x (Thermo Fisher Scientific, Waltham-MA, USA). Charge state deconvolution and deisotoping were not performed. The raw data was processed using Proteome Discoverer (version 2.x, Thermo Scientific). MS2 spectra were searched with SEQUEST engine against a database of *P. pseudoalcaligenes* CECT5344 (deposited

in the EMBL database under the accession number HG916826). Peptides were generated from a tryptic digestion with up to one missed cleavages, carbamidomethylation of cysteines as fixed modifications, and oxidation of methionine as variable modifications. Precursor mass tolerance was 10 ppm and product ions were searched at 0.8 Da tolerances. Peptide spectral matches (PSM) were validated using percolator based on q-values at 1% FDR (False Discovery Rate), calculated against concatenated decoy database. With Proteome Discoverer, peptide identifications were grouped into proteins according to the law of parsimony and filtered to 1% FDR. For proteins identified from only one peptide, fragmentations were checked manually.

4.6. Bioinformatics and statistics

The bioinformatic analysis of protein sequences included computational predictions of subcellular localization that were carried out using the PSORTb program version 3.0.2. (http://www.psort.org/psortb/index.html). Proteins identified by LC-MS/MS were quantified by using the Progenesis IQ software, as follows: the raw data were imported to the software and an automatic processing of the data was performed, using a relative quantification that considers the three most abundant peptides. After, the most suitable run was automatically selected as alignment reference and some parameters were set up, including peak picking limits (by deleting ions with a charge less than one and higher than four) and the retention time limits (only ions with retention time between five minutes and 75 minutes were considered). Once the alignment was run, it was reviewed to ensure a high alignment quality. Several experimental designs were carried out to compare the proteome of the wild-type strain and *nitA*$^{-}$ and *nitC*$^{-}$ mutant strains (Fig. 5).

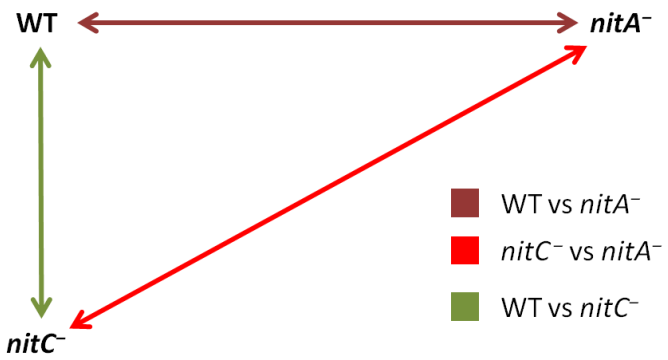

Figure 5. Experimental designs developed by using Progenesis QI software. Each arrow represents an experimental design.

The following step was to filter proteins considering a *p*-value (Anova) ≤ 0.05 and a fold change ≥ 2 for each experimental design.

STRING software version 10.0 (Szklarczyk *et al.,* 2015) was applied to identify interactions between proteins by using the *Pseudomonas mendocina* NK01 database.

MEGA7 software (Kumar *et al.,* 2015) was used to build phylogenetic trees considering the amino acid sequence of the protein for different species of bacteria against *P. pseudoalcaligenes* CECT5344. These sequences were obtained from NCBI by protein BLAST. The trees were built by using the UPGMA method by aligning the sequences previously.

The genetic context of *P. pseudoalcaligenes* CECT5344 was analyzed by utilizing the KEGG database (Kanehisa *et al.,* 2016).

All the presented data correspond to three independent experiments. Some graphs have standard deviations included and other results are shown as one representative experiment.

5. Results

5.1. BN-PAGE of soluble fraction of *P. pseudoalcaligenes* CECT5344

To identify protein complexes involved in cyanide assimilation in *P. pseudoalcaligenes* CECT5344, the BN-PAGE technique has been carried out and optimized. Three experimental replicates, consisting of two different biological samples and from one of them, two methodological replicates, have been performed in each condition. The gels were analyzed to find vertically aligned spots differentially expressed.

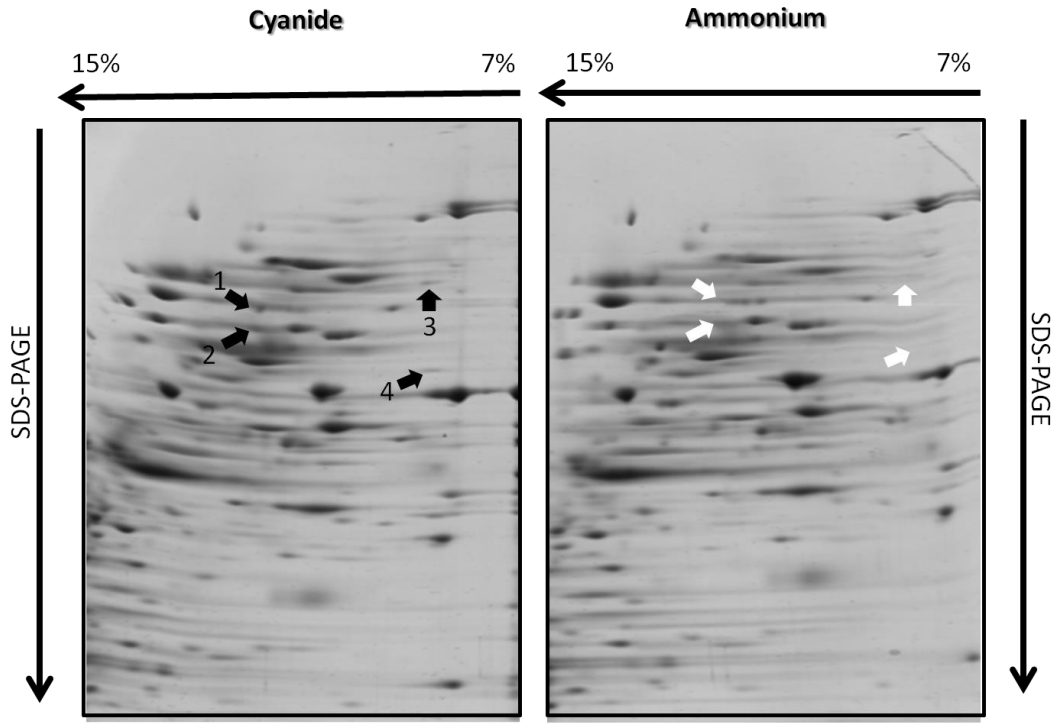

Figure 6. BN-PAGE analysis of soluble fractions of *P. pseudoalcaligenes* CECT5344 grown with cyanide or ammonium. Soluble fractions were obtained as described in Materials and Methods section. Black and white arrows indicate presence or absence of spots, respectively. One representative gel of the three replicates for each N source is shown.

The spots that were aligned vertically (spots 1 and 2 and spots 3 and 4) in the gels carried out with soluble fractions from cells grown with cyanide were excised and analyzed by MALDI/TOF-TOF (SCAI, UCO). In addition to aligned proteins, the BN-PAGE analysis showed other three non-aligned spots induced by cyanide and one repressed. These spots were also identified by MALDI-TOF/TOF (Supplementary Material Fig. S1 and Table S1).

The data for identification of spots 1 and 2 forming the complex I, and the spots 3 and 4 that constitute the complex II, are shown in Table 3.

Table 3. Identification of protein complexes induced by cyanide.

Spot Nº	Protein name	Accession number *	Score C.I. %	Score	P.I.	Molecular weight(Da)	
1	Phosphoenolpyruvate synthase	W6QUW7	100	290	5.35	94250	Complex I
2	Chaperone protein DnaK	W6RCA2	100	191	4.8	68718.3	
3	Phosphoenolpyruvate carboxylase	W6QT92	99,975	81	5.83	97739	Complex II
4	Pyruvate carboxylase subunit B	W6R3U1	100	188	5.48	65766.9	

(*) Accession number according to Luque-Almagro and *et al.,* (2013).

Three of these four proteins are enzymes that participate in carbon metabolism: phosphoenolpyruvate synthase catalyzes the phosphorilation of pyruvate to produce phosphoenolpyruvate; phosphoenolpyruvate carboxilase catalyzes the conversion of phosphoenolpyruvate into oxaloacetate and pyruvate carboxylase catalyzes the conversion of pyruvate into oxaloacetate (Cooper and Kornberg, 1967; Kai *et al.* 2003; Mathews *et al.,* 2003);

The phosphoenolpyruvate synthase *locus* presents some neighbor genes that encode enzymes such as aconitate hydratase (BN5_2137) or 2-methylcytrate synthase (BN5_2139) related to carbon metabolism (Fig. 7).

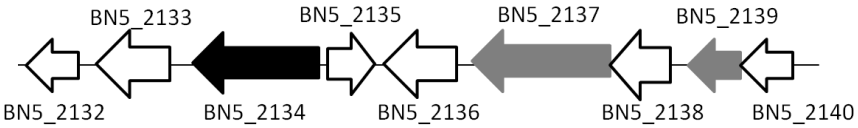

Figure 7. Phosphoenolpyruvate synthase gene cluster of *P. pseudoalcaligenes* CECT5344. The phosphoenolpyruvate synthase gene (BN5_2134) is shown in black; the aconitase hydratase gene (BN5_2137) and the methylcytrate synthase gene (BN5_2139) are shown in grey and the other genes are shown in white.

The *dnaK* gene (BN5_0910) coding for the chaperone protein (spot 2) could be part of an operon as described in *Streptomyces coelicolor* (Bucca *et al.,* 2003), which also

involves the *grpE* and *dnaJ* genes. These genes are also present in *P. pseudoalcaligenes* CECT5344 (BN5_0909 and BN5_0911, respectively). In addition, the *dapB* gene that encodes the dihydropicolinate reductase (BN5_0912) is also present in this locus (Fig. 8). Dihydropicolinate reductase together with dihydropicolinate synthase catalyzes the biosynthesis of lysine (Fig. 9).

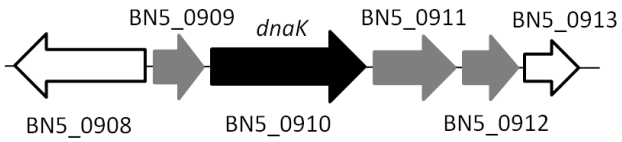

Figure 8. *dnaK* chaperone gene cluster of *P. pseudoalcaligenes* CECT5344. The *dnaK* gene (BN5_0910) is shown in black; the *grpE* (BN5_0909), the *dnaJ* (BN5_0911) and the *dapB* (BN5_0912) genes are shown in grey, and other genes are shown in white.

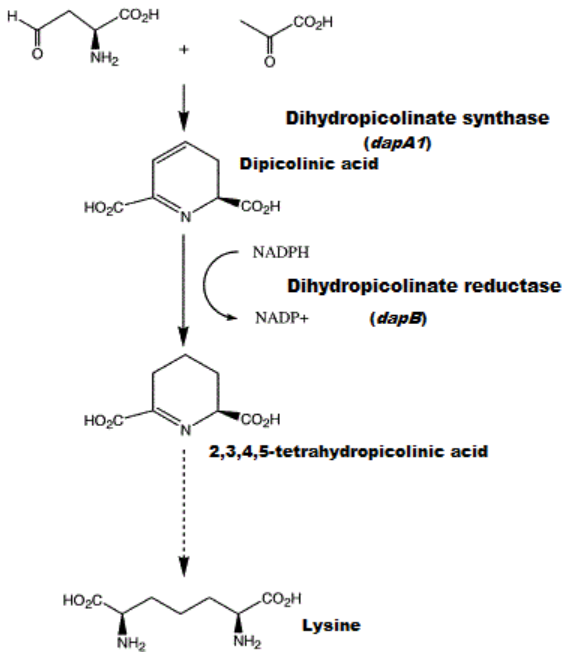

Figure 9. Biosynthetic pathway of lysine. (Paiva *et al.,* 2001).

In order to identify possible relationships with proteins from complexes I and II, these proteins were analyzed by the STRING software. The interaction analysis of phosphoenolpyruvate carboxylase and pyruvate carboxylase (subunit B) showed an indirect relationship between these two proteins through the subunit A of pyruvate

carboxylase. Phosphoenolpyruvate carboxylase also interacts with phosphoenolpyruvate synthase, as well as with two malate:quinone oxidoreductases (Fig. 10). Phosphoenolpyruvate carboxylase participates with 122 other proteins in the carbon metabolism and with 47 other proteins in pyruvate metabolism.

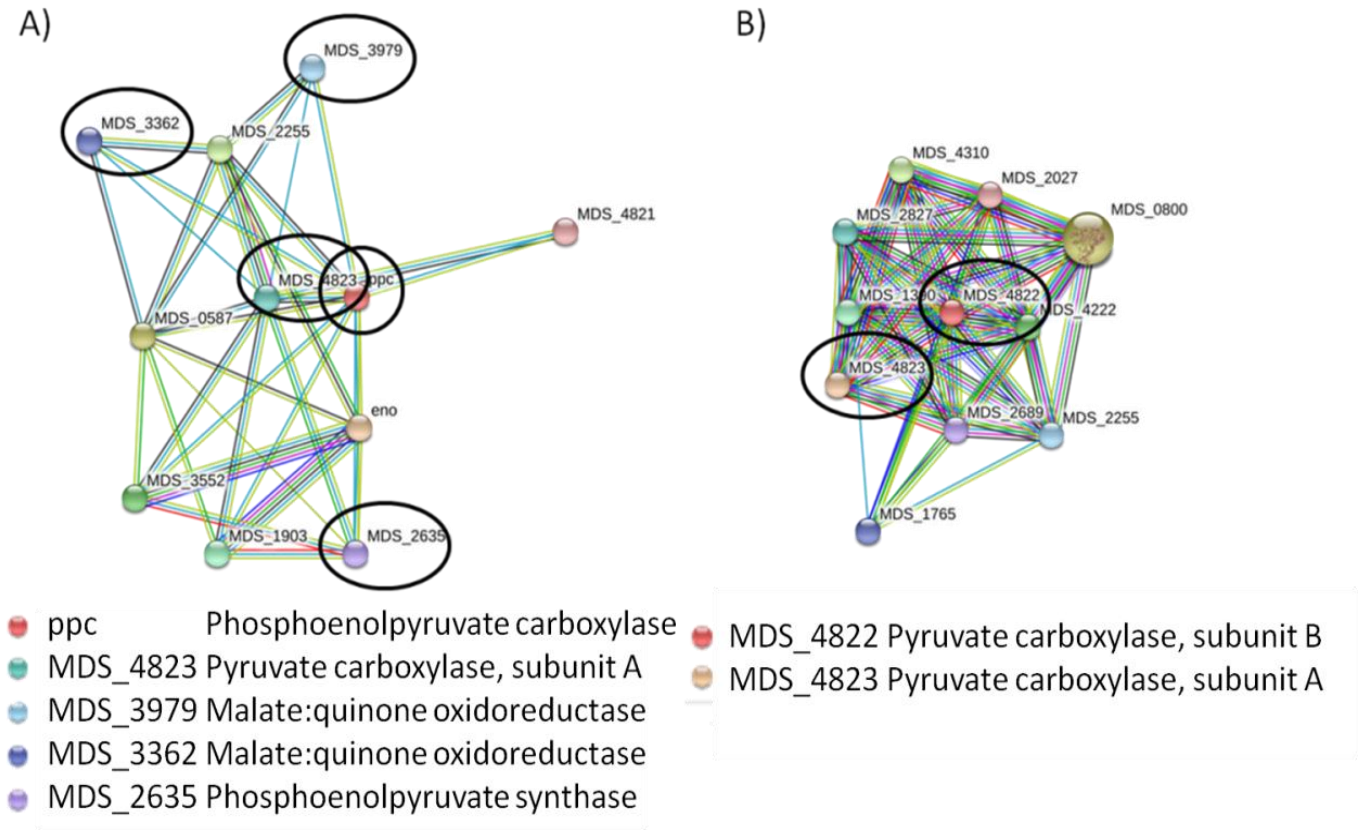

Figure 10. Interaction analysis of phosphoenolpyruvate carboxylase and pyruvate carboxylase, subunit B. This analysis was performed with the STRING software (v. 10.0) by choosing the *Pseudomonas mendocina* NK-01 database. (A) phosphoenolpyruvate carboxylase and (B) pyruvate carboxylase, subunit B.

5.2. Characterization of *nitA*⁻ and *nitC*⁻ *P. pseudoalcaligenes* CECT5344

5.2.1. Bacterial Growth

The *nitA*⁻ and *nitC*⁻ mutant strains of *P. pseudoalcaligenes* CECT5344 were cultured in M9 minimal medium with 50 mM acetate as carbon source and 2 mM ammonium as nitrogen source. After 24 hours, when ammonium was depleted, 2 mM sodium cyanide or 2 mM ammonium chloride was added.

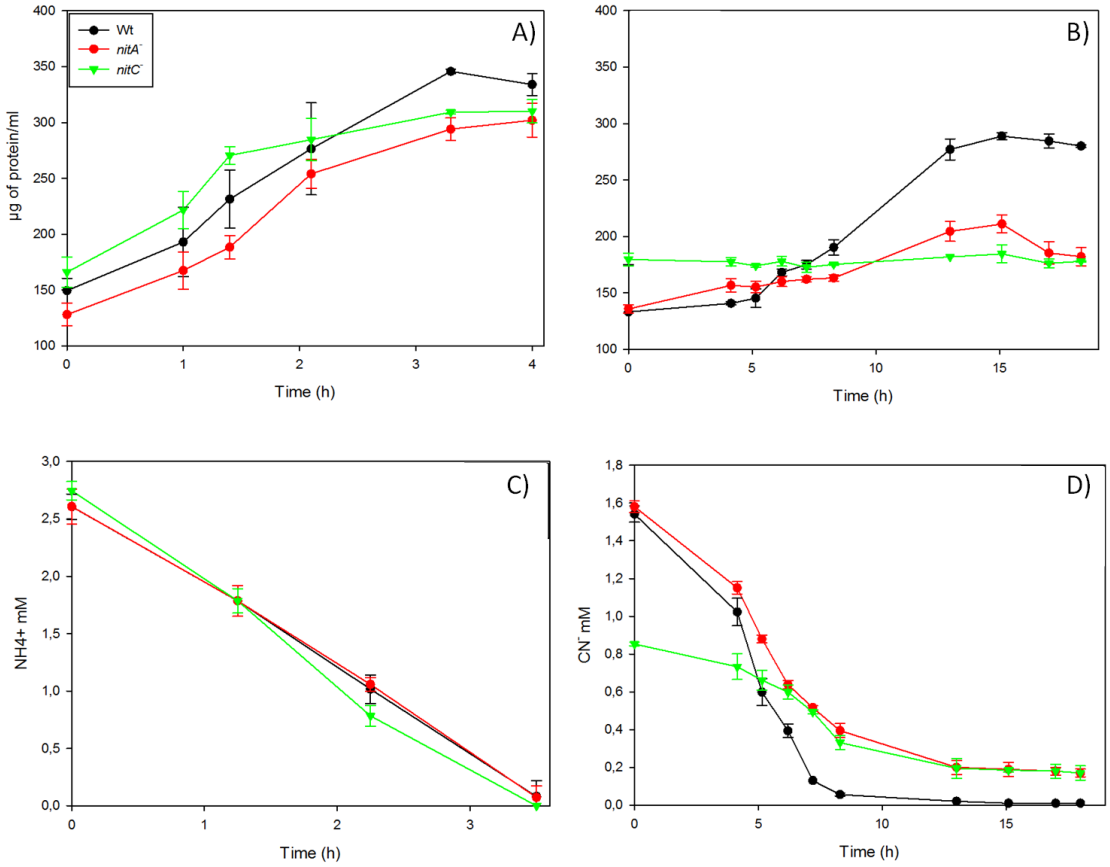

Figure 11. Growth and N-source uptake of the wild-type and *nitA*⁻ and *nitC*⁻ mutant strains of *P. pseudoalcaligenes* CECT5344 with different nitrogen sources. Ammonium (A,C) or cyanide (B,D) were added as nitrogen source. Bacterial growth was measured by determining the protein concentration (A,B). Ammonium concentration (C) or cyanide concentration (D) were measured as indicated in Materials and Methods section.

Bacterial strains showed a similar growth with ammonium (Fig. 11A). By contrast, the wild type strain showed significant growth with cyanide, whereas the *nitA*⁻ and *nitC*⁻

mutant strains did not grow (Fig. 11B). Regarding to the consumption of the nitrogen source, ammonium was similarly consumed by all four strains (Fig. 11C). However, extracellular cyanide decreased totally in cultures inoculated with the wild type strain, but not in the cultures with *nitA*$^-$ and *nitC*$^-$ mutants (Fig. 11D). The partial consumption of cyanide in the mutant strains is probably due to chemical reactions between cyanide and 2-oxoacids (Estepa *et al.,* 2012), which generate cyanohydrins (nitriles) that are not assimilated by the mutant strain.

5.2.2. Nitrilase activity assay

The nitrilase activity was assayed in whole cells of the *nitA*$^-$ and *nitC*$^-$ mutants of *P. pseudoalcaligenes* CECT5344 grown with ammonium or sodium cyanide as nitrogen source. Both the wild-type and the *nitA*$^-$ and *nitC*$^-$ mutants showed similar low levels of nitrilase activity when cells were grown with ammonium (not shown). However In the *nitA*$^-$ and *nitC*$^-$ mutants this activity was very low when cells were cultured with cyanide, whereas under cyanotrophic conditions the wild-type strain showed a very high nitrilase activity (Fig. 12).

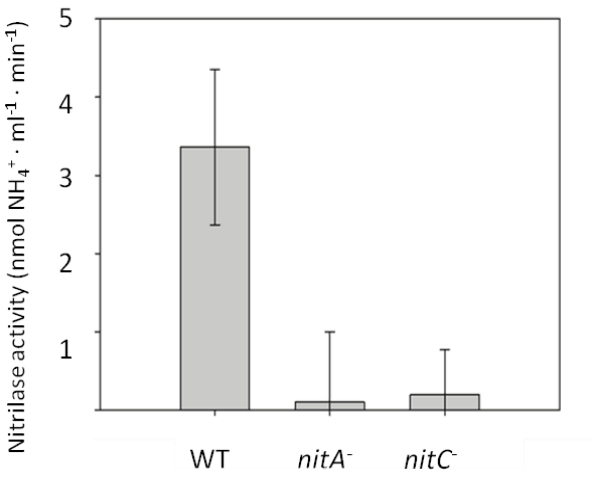

Figure 12. Nitrilase activity in the wild-type strain and the *nitA*$^-$ and *nitC*$^-$ mutants of *P. pseudoalcaligenes* CECT5344.

5.2.3. Proteomic analysis (LC-MS/MS)

The *P. pseudoalcaligenes* mutants defective in *nitA*⁻ and *nitC*⁻ genes were analyzed by gel-free quantitative proteomic analysis. These mutant strains, as well as the wild-type strain, were cultured in M9 minimal medium (pH 9.5) with 50 mM sodium acetate as carbon source and 2 mM sodium cyanide as nitrogen source. Cells were harvested at the mid-exponential growth phase (A_{600} ˜0.4), when about 30% of cyanide remained in the media. Soluble fractions were obtained as described in Material and Methods section and proteins were cleaned up, digested and further analyzed by LC-MS/MS.

In a comparative experimental design carried out between the wild-type and the *nitA*⁻ mutant strain, 28 proteins were induced in the *nitA*⁻ mutant (Table 4). Proteins involved in L-arginine degradation via ADI pathway (arginine deiminase, W6R686) and coenzyme A biosynthesis (dephospho-CoA kinase, W6QQS7) were found to be induced in the *nitA*⁻ mutant strain. Among the induced proteins, two CRISPR-associated proteins (W6QR33 and W6QZ01) were also identified (Table 4). In addition, the regulatory Pha (phasin) protein (W6R8A0) a protein involved in polyhydroxyalkanoate metabolism, was induced by cyanide in the *nitA*⁻ strain. The Pha protein was also found induced in the *nitC*⁻ mutant strain (Table 6).

In the Supplementary material 2 are shown the Tables S2 and S3 corresponding to the experimental design where *nitA*⁻ and *nitC*⁻ mutants were compared.

Table 4. Induced proteins in the *nitA*$^{-}$ mutant strain compared to the wild-type strain under cyanotrophic conditions.

Protein accession number[1]	Gene accession number[2]	*p*-value	F.C.[3]	Description
W6QS57	BN5_0728	0,000	9,261	Glutamyl-tRNA(Gln) amidotransferase subunit A
W6RKA7	BN5_3677	0,021	5,336	50S ribosomal protein L15
W6QYR0	BN5_0639	0,003	4,965	Uncharacterized protein
W6QY01	BN5_2787	0,020	4,882	NAD(P)H dehydrogenase (quinone)
W6R5F1	BN5_3049	0,015	4,703	Glyceraldehyde-3-phosphate dehydrogenase
W6QRJ2	BN5_0933	0,043	4,663	30S ribosomal protein S15
W6R347	BN5_2205	0,041	4,592	Hydroxysteroid dehydrogenase-like protein 2
W6R1G3	BN5_3561	0,048	4,324	Transcriptional regulator
W6QWI2	BN5_1762	0,003	3,721	Peptidyl-prolyl cis-trans isomerase
W6R1Z2	BN5_3706	0,034	3,535	50S ribosomal protein L1
W6QR33	BN5_0771	0,045	3,423	CRISPR-associated Cas5e family protein
W6RLT4	BN5_4300	0,019	3,327	Uncharacterized protein
W6R110	BN5_1506	0,033	3,050	Uncharacterized protein
W6RI94	BN5_2964	0,009	3,023	Isochorismatase hydrolase
W6R686	BN5_3331	0,029	2,881	Arginine deiminase
W6QZ01	BN5_0772	0,024	2,830	CRISPR-associated Cse3 family protein
W6R6B8	BN5_3373	0,049	2,623	Peptidyl-tRNA hydrolase
W6R0J9	BN5_3685	0,008	2,421	50S ribosomal protein L24
W6QQN7	BN5_0208	0,029	2,408	Peptidyl-prolyl cis-trans isomerase
W6QUL4	BN5_1076	0,023	2,233	50S ribosomal protein L19
W6QQS7	BN5_0661	0,041	2,190	Dephospho-CoA kinase
W6R8A0	BN5_4096	0,004	2,175	Phasin-like protein
W6QW47	BN5_2161	0,019	2,161	ABC transporter ATP-binding protein
W6R187	BN5_3481	0,025	2,141	Ubiquinol-cytochrome c reductase iron-sulfur subunit
W6QXH7	BN5_2627	0,035	2,099	Chemotaxis response regulator protein-glutamate methylesterase
W6RKX0	BN5_3982	0,001	2,025	Uncharacterized protein
W6QPC7	BN5_0176	0,004	2,009	Mg chelatase, subunit ChlI
W6RC90	BN5_0895	0,030	2,006	Glutathione peroxidase

[1]Accession number from UniProt and [2]Accession number from GenBank (Luque-Almagro *et al.,* 2013); [3]Fold Change. Only proteins with a *p*-value ≤ 0.05 and a fold change ≥ 2 were considered.

The sequence of the whole genome of the CECT5344 strain has been used to identify the genes encoding the most relevant proteins induced in the *nitA*$^-$ mutant strain (Table 4, Fig. 13). The arginine deiminase gene clustered together other genes involved in arginine metabolism (ornithine carbamoyltransferase, BN5_3332; arginine/ornithine antiporter, BN5_3330 and carbamate kinase, BN5_3333). The gene coding for isochorismate hydrolase (also named nicotinamidase) is located close to genes related to nicotinamide and nicotinate metabolism (nicotinate phosphoribosyltransferase, BN5_2965 and NAD^+ synthetase, BN5_2966). The two CRISPR genes induced by cyanide were also clustered together (Fig. 13).

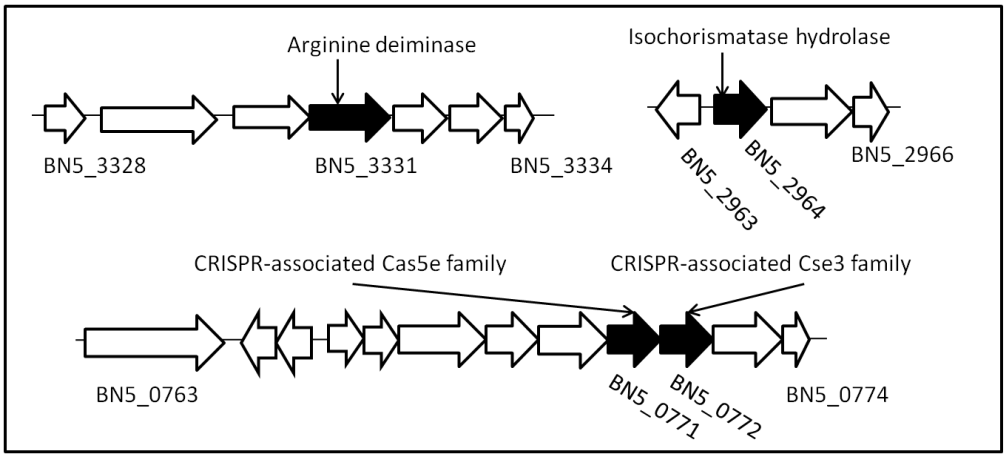

Figure 13. Position in the genome of some genes encoding proteins shown in Table 4 that are specifically induced in the *nitA*$^-$ mutant.

The *phaP* gene (BN5_4096), which codes for a phasin that is involved in the formation of granules of polyhydroxyalkanoates (PHA) with high number of carbon atoms (Pötter *et al.,* 2002; Manso *et al.,* 2015), is found in the genome of *P. pseudoalcaligenes* CECT5344 next to other genes related to PHA metabolism such as the polyhydroxyalkanoate synthase (BN5_4097), the repressor *phaR* gene (BN5_4095) and the poly-3-hydroxyalkanoate synthase gene (BN5_4097). Another gene cluster also involved in PHA metabolism is located near this *locus* and is composed of an transcription activator gene for short chain PHA (polyhydroxybutyrate) synthesis (*phbR,* BN5_4102), an acetoacetyl-CoA reductase gene (*phaB,* BN5_4103), an acetyl-CoA

acetyltransferase gene (*phaA3,* BN5_4104) and a poly(R)-hydroxyalkanoic acid synthase, class I gene (*phaC5,* BN5_4105).

At least 55 proteins were repressed in the *nitA*$^-$ mutant strain compared to the wild-type strain, including five proteins encoded by the *nit1C* gene cluster, NitC (H9N5E1), NitB (H9N5D2), NitH (H9N5D8), NitG (H9N5E9) and NitD (H9N5E3), as well as a malate:quinone oxidoreductase (W6RC63) (Table 5). Other proteins involved in glycine, arginine threonine or histidine biosynthetic pathways were also repressed such as serine hydroxymethyltransferase (W6QT19), *N*-acetyl-gamma-glutamyl-phosphate reductase (W6QZP2), histidinol dehydrogenase (W6R1A2), and threonine synthase (W6QUM0). Other proteins repressed in the *nitA*$^-$ mutant were an oxidoreductase FAD/NAD(P) binding subunit (W6QXM5), a multidrug resistance protein (W6RDI9) and a cytochrome *c* oxidase, *cbb*3-type (Table 5).

Table 5. Repressed proteins in the *nitA*$^-$ mutant strain compared to the wild-type strain under cyanotrophic conditions.

Protein accession number[1]	Gene accession number[2]	*p*-value	F.C.[3]	Description
H9N5E3	BN5_1633	0,003	1513,047	Radical SAM domain-containing protein (NitD)
H9N5D9	BN5_1636	0,000	166,952	Uncharacterized protein (NitG)
W6QXC9	BN5_2076	0,045	55,375	Transcriptional activator CopR
H9N5D8	BN5_1637	0,003	22,670	FAD dependent oxidoreductase (NitH)
W6RAC3	BN5_0149	0,018	15,981	Putative endoribonuclease L-PSP
W6QZP2	BN5_3732	0,017	15,409	N-acetyl-gamma-glutamyl-phosphate reductase
W6RBR8	BN5_0665	0,028	12,699	Fimbrillin
W6R0Q0	BN5_4131	0,001	12,328	Putative capsule polysaccharide export protein
W6QVZ5	BN5_2095	0,014	11,629	Outer membrane porin, OprD family
W6QXM5	BN5_3063	0,048	11,006	Oxidoreductase FAD/NAD(P)-binding subunit
H9N5E2	BN5_1631	0,000	8,099	Uncharacterized protein (NitB)
H9N5E1	BN5_1632	0,000	7,982	Nitrilase (NitC)
W6QVB2	BN5_1327	0,001	7,018	Outer membrane protein OprJ
W6R184	BN5_3476	0,002	6,892	Transport-associated
W6RDK8	BN5_1353	0,009	6,665	Protein CcoG
W6QS54	BN5_1163	0,033	5,552	Iron-regulated protein A
W6RDI9	BN5_1328	0,030	5,248	Multidrug resistance protein MdtF
W6RCD4	BN5_0947	0,016	4,516	Two-component response regulator CbrB
W6REY3	BN5_1853	0,049	4,382	Isocitrate lyase
W6R020	BN5_3044	0,026	4,245	Peptidyl-prolyl cis-trans isomerase
W6QSD2	BN5_0279	0,040	4,002	Osmolarity response regulator
W6QWR4	BN5_2373	0,039	3,989	Electron-transferring-flavoproteindehydrogenase
W6RC63	BN5_0860	0,039	3,825	Probable malate:quinone oxidoreductase
W6QXP9	BN5_2187	0,041	3,631	Exonuclease
W6QVW1	BN5_2446	0,016	3,543	Cytochrome c oxidase, cbb3-type, subunit II
W6QS37	BN5_0708	0,033	3,500	Uncharacterized protein
W6QXN7	BN5_3079	0,000	3,498	OmpA domain-containing protein
W6RKG9	BN5_3726	0,046	3,479	Tyrosine--tRNA ligase
W6QXZ2	BN5_3174	0,007	3,295	Uncharacterized protein
W6R1T3	BN5_4158	0,004	3,076	Sulfate-binding protein
W6QZD9	BN5_0934	0,044	3,034	Polyribonucleotide nucleotidyltransferase
W6QV73	BN5_1791	0,002	3,015	Methyl-accepting chemotaxis protein II
W6QUM0	BN5_1081	0,034	2,983	Threonine synthase

W6QSL8	BN5_1329	0,015	2,947	Multidrug resistance protein A
W6R3G9	BN5_2367	0,001	2,920	Extracellular solute-binding protein
W6R591	BN5_2991	0,015	2,918	High-affinity branched-chain amino acid transport ATP-binding protein
W6QYX9	BN5_0737	0,025	2,877	Peptidase U62, modulator of DNA gyrase
W6RJ15	BN5_3203	0,004	2,725	Isochorismatase hydrolase
W6QVG9	BN5_1382	0,013	2,681	DNA topoisomerase 1
W6QST4	BN5_0439	0,013	2,628	ABC-type transporter periplasmic component protein
W6QYV0	BN5_3096	0,015	2,582	Porin D
W6QSI1	BN5_0334	0,017	2,341	Methyl-accepting chemotaxis protein I
W6QWF0	BN5_2246	0,025	2,340	Uncharacterized protein
W6QU53	BN5_1854	0,000	2,296	Uncharacterized protein
W6QTI9	BN5_0646	0,004	2,260	Serine hydroxymethyltransferase
W6QXN5	BN5_0312	0,003	2,234	Methyl-accepting chemotaxis sensory transducer
W6RGC5	BN5_2365	0,042	2,231	OmpA/MotB domain-containing protein
W6QW62	BN5_1647	0,012	2,147	ATP-dependent Clp protease ATP-binding subunit ClpC
W6R4T8	BN5_2826	0,027	2,138	Outer membrane protein assembly factor BamA
W6QSL9	BN5_0888	0,047	2,122	OmpA/MotB domain-containing protein
W6R473	BN5_4434	0,046	2,119	Peptide methionine sulfoxide reductase MsrA
W6R0U2	BN5_3769	0,016	2,105	LPS-assembly protein LptD
W6QZM4	BN5_3703	0,048	2,017	DNA-directed RNA polymerase subunit beta
W6QWA0	BN5_1657	0,003	2,016	Lipoprotein heavy metal/multidrug efflux protein
W6R1A2	BN5_3496	0,021	2,007	Histidinol dehydrogenase

[1]Accession number from UniProt and [2]Accession number from GenBank (Luque-Almagro *et al.*, 2013). [3]Fold Change. Only proteins with a *p*-value ≤ 0.05 and a fold change ≥ 2 were considered.

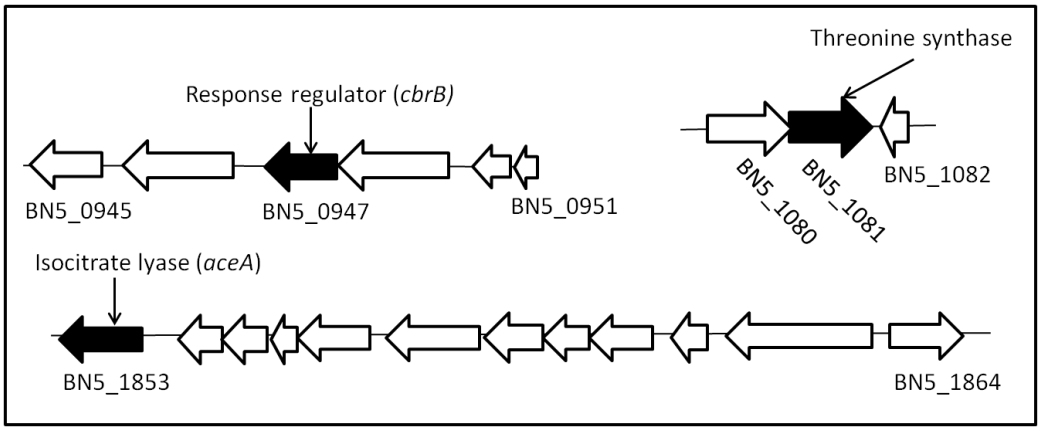

Figure 14. Position in the genome of genes encoding proteins shown in Table 5 that are specifically repressed in the *nitA*⁻ mutant strain.

Some genes that code for proteins repressed in the *nitA*⁻ mutant are arranged in gene clusters (Figs. 14). Thus, the threonine synthase forms a cluster with homoserine dehydrogenase (BN5_1080). The *cbrB* gene constitutes a cluster with *cbrA* (BN5_0948) whose product is a two-component sensor kinase. Also the isocitrate lyase (BN5_1853),

an adenylosuccinate lyase (BN5_1858), and two isocitrate dehydrogenases (BN5_1863 and BN5_1864) are present in the same *locus*. Multidrug resistance gene (*mexD,* BN5-1328) cluster together *oprJ* gene (BN5_1327) that codes for the outer membrane protein and the *mexC* (BN5_1329)*,* encoding is a multidrug resistance protein A. The subunit II of the cytochrome *c* oxidase *cbb*$_3$-type gene (BN5_2446) shares *locus* with more subunits. The multidrug resistance protein Mdt7 and the cytochrome *c* oxidase *cbb*$_3$-type were also repressed in the *nitC*$^-$ strain (Table 7).

The comparative experimental design between the wild-type strain and the *nitC*$^-$ mutant strain revealed that 91 proteins were induced by cyanide in the *nitC*$^-$ mutant strain. Five enzymes involved in amino acid biosynthesis were induced in the *nitC*$^-$ mutant strain, including carbamil-phosphate synthase small chain (W6RCA6), ATP phosphoribosyltransferase (W6RJQ4), dihydroxy-acid dehydratase (W6RL00), homoserine kinase (W6QRT8), tryptophan synthase alpha chain (W6QQ93) and *S*-adenosylmethionine synthase (W6RAS5) (Table 6). Another proteins also induced in the *nitC*$^-$ mutant were, threonylcarbamoyl-AMP synthase (W6QWW4), fumarate hydratase (W6RE08), hydrogen peroxide-inducible genes activator (W6RLM3), hydroxyacylglutathione hydrolase (W6RG04) and gluthatione peroxidase (W6RC90).

Table 6. LC-MS/MS analysis of the wild-type strain compared to the *nitC*⁻ mutant strain. Cyanide induced proteins in the *nitC*⁻ strain are shown.

Protein accession number[1]	Gene accession number[2]	*p* -value	F.C.[3]	Description
W6QRT8	BN5_0102	0,034	25,587	Homoserine kinase
W6R1T8	BN5_4163	0,016	8,008	Putative aliphatic sulfonates-binding protein
W6QPA6	BN5_0150	0,001	7,851	Cytochrome C6
W6QYG3	BN5_0579	0,006	7,558	Urease subunit beta
W6RI94	BN5_2964	0,002	6,595	Isochorismatase hydrolase
W6QRK3	BN5_0518	0,026	6,471	N-acetylmuramoyl-L-alanine amidase
W6RG04	BN5_2218	0,013	5,284	Hydroxyacylglutathione hydrolase
W6QVJ2	BN5_2319	0,014	5,032	Uncharacterized protein
W6QRJ2	BN5_0933	0,036	5,030	30S ribosomal protein S15
W6QRB3	BN5_0856	0,024	4,859	50S ribosomal protein L27
W6RJM8	BN5_3477	0,009	4,716	ClpXP protease specificity-enhancing factor
W6RDZ3	BN5_1509	0,002	4,677	Arc
W6QWW4	BN5_0030	0,010	4,605	Threonylcarbamoyl-AMP synthase
W6QX60	BN5_2518	0,004	4,491	Metallo-beta-lactamase family protein
W6QUU3	BN5_2114	0,013	4,400	Nitrate transporter periplasmic component
W6R1J6	BN5_3601	0,032	4,288	Inorganic pyrophosphatase
W6R0B8	BN5_3142	0,022	4,221	Peptidyl-prolyl cis-trans isomerase
W6QTJ9	BN5_0664	0,025	4,218	Type 4 fimbrial biogenesis protein PilB
W6RM46	BN5_4445	0,004	4,172	Glutaredoxin
W6RBC9	BN5_0552	0,011	4,166	Urease accessory protein UreG
W6RKA7	BN5_3677	0,008	4,159	50S ribosomal protein L15
W6R445	BN5_2581	0,032	4,144	Peptidylprolyl isomerase
W6QRT1	BN5_0600	0,013	3,926	DNA-binding protein Fis
W6RLM3	BN5_4225	0,038	3,832	Hydrogen peroxide-inducible genes activator
W6QSY1	BN5_0484	0,005	3,817	Bifunctional protein HldE
W6QWY7	BN5_2815	0,006	3,709	2-dehydro-3-deoxyphosphooctonate aldolase
W6R8A0	BN5_4096	0,004	3,676	Phasin-like protein
W6R1Y1	BN5_3696	0,034	3,528	50S ribosomal protein L3
W6R9C0	BN5_4452	0,006	3,478	Alkyl hydroperoxide reductase AhpD
W6R2N9	BN5_4433	0,041	3,366	Peptide methionine sulfoxide reductase MsrB
W6QW42	BN5_2540	0,033	3,361	Sulfurtransferase TusA homolog
W6QZE7	BN5_3261	0,004	3,356	Nucleoside diphosphate kinase
W6RKV8	BN5_3962	0,030	3,315	Nitrogen regulation protein NR(I)
W6R1A4	BN5_3960	0,021	3,299	Uncharacterized protein
W6RKY6	BN5_4002	0,024	3,226	Gamma-glutamyltranspeptidase
W6QQN7	BN5_0208	0,001	3,220	Peptidyl-prolyl cis-trans isomerase
W6RE08	BN5_1524	0,006	3,217	Fumarate hydratase class II
W6R9D4	BN5_4467	0,030	3,204	DNA-invertase
W6QSF0	BN5_0823	0,008	3,099	Uncharacterized protein
W6RJS0	BN5_3512	0,019	2,996	PTS IIA-like nitrogen-regulatory protein PtsN
W6QXS7	BN5_3119	0,007	2,966	Putative quercetin 2,3-dioxygenase PA3240
W6QXL3	BN5_0277	0,042	2,956	Phenylacetic acid degradation-related protein
W6QW47	BN5_2161	0,025	2,935	ABC transporter ATP-binding protein
W6R563	BN5_2966	0,044	2,932	NH(3)-dependent NAD(+) synthetase
W6RL00	BN5_4017	0,008	2,929	Dihydroxy-acid dehydratase
W6R0J9	BN5_3685	0,009	2,890	50S ribosomal protein L24
W6QSJ5	BN5_0349	0,031	2,809	Fructose-bisphosphate aldolase, class II
W6R7C1	BN5_3694	0,013	2,807	50S ribosomal protein L23
W6R2R6	BN5_4453	0,011	2,803	Uncharacterized protein

W6R132	BN5_1526	0,010	2,792	Uncharacterized protein
W6RFX0	BN5_2178	0,012	2,771	Succinate dehydrogenase, iron-sulfur protein
W6R6B8	BN5_3373	0,047	2,763	Peptidyl-tRNA hydrolase
W6QXC5	BN5_0151	0,011	2,756	Flavin monoamine oxidase-related protein
W6QUC9	BN5_1488	0,006	2,675	Arginine/ornithine transport protein AotP
W6RKF5	BN5_3697	0,032	2,662	30S ribosomal protein S10
W6RJA0	BN5_3324	0,028	2,657	Uncharacterized protein
W6QV68	BN5_2194	0,008	2,605	Peptide methionine sulfoxide reductase MsrB
W6RFW4	BN5_2173	0,047	2,597	Succinate--CoA ligase [ADP-forming] subunit alpha
W6QST4	BN5_0439	0,001	2,594	ABC-type transporter periplasmic component protein
W6R242	BN5_4228	0,000	2,585	Uncharacterized protein
W6R1L4	BN5_3621	0,044	2,579	2-hydroxymuconic semialdehyde dehydrogenase
W6QV43	BN5_1257	0,029	2,522	Probable transcriptional regulatory protein BN5_1257
W6QT34	BN5_0536	0,012	2,503	30S ribosomal protein S18
W6RCA6	BN5_0915	0,006	2,490	Carbamoyl-phosphate synthase small chain
W6QXM0	BN5_3058	0,015	2,463	FMN-dependent NADH-azoreductase
W6QZ60	BN5_2720	0,029	2,462	Alkyl hydroperoxide reductase
W6RLT4	BN5_4300	0,014	2,459	Uncharacterized protein
W6R1B7	BN5_3511	0,009	2,429	SSU ribosomal protein S30P / sigma 54 modulation protein
W6QQ93	BN5_0046	0,031	2,424	Tryptophan synthase alpha chain
W6QXY8	BN5_0417	0,006	2,419	ATP-dependent protease subunit HslV
W6QZH6	BN5_2848	0,002	2,416	Cold shock protein (Beta-ribbon, CspA family)
W6RLQ8	BN5_4275	0,003	2,413	31 kDa immunogenic protein
W6R3B3	BN5_2295	0,024	2,391	MarR family transcriptional regulator
W6QQM4	BN5_0193	0,000	2,293	Nucleoside diphosphate kinase regulator
W6QPP2	BN5_0301	0,004	2,278	Beta-ketoacyl synthase
W6R5J2	BN5_3080	0,022	2,271	Protein TolB
W6RAS5	BN5_0340	0,028	2,270	S-adenosylmethionine synthase
W6R268	BN5_3796	0,020	2,261	Uncharacterized protein
W6R187	BN5_3481	0,004	2,259	Ubiquinol-cytochrome c reductase iron-sulfur subunit
W6QSF7	BN5_0309	0,007	2,256	Response regulator receiver protein
W6QZS8	BN5_1079	0,028	2,215	Thiol:disulfide interchange protein DsbC
W6RJQ4	BN5_3497	0,009	2,153	ATP phosphoribosyltransferase
W6R0I0	BN5_4063	0,007	2,150	Uncharacterized protein
W6R2Y2	BN5_2160	0,024	2,150	Arylesterase
W6RKX0	BN5_3982	0,014	2,140	Uncharacterized protein
W6QX33	BN5_2493	0,011	2,107	MarR family transcriptional regulator
W6QQB9	BN5_0538	0,038	2,101	50S ribosomal protein L9
W6QTL3	BN5_1215	0,043	2,058	Hydroxyacylglutathione hydrolase
W6RC90	BN5_0895	0,047	2,044	Glutathione peroxidase
W6R936	BN5_4362	0,045	2,011	Uncharacterized protein in lpd-3 5'region

[1]Accession number from UniProt and [2]Accession number from GenBank (Luque-Almagro *et al.,* 2013). [3]Fold Change. Only proteins with a *p*-value ≤ 0.05 and a fold change ≥ 2 were considered.

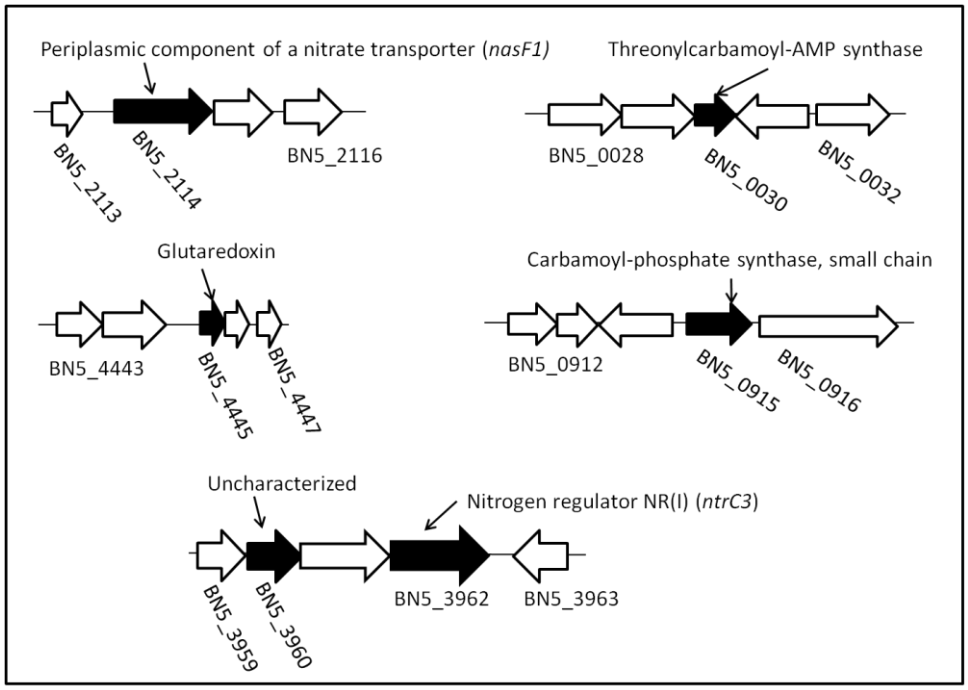

Figure 15. *Loci* of some genes encoding proteins specifically induced in the *nitC*$^-$ shown in Table 6.

Some gene cluster arrangements of genes that encoding relevant proteins shown in Table 6 are represented in Figure 15, including a gen coding for the periplasmic component of a nitrate transporter (*nasF1,* BN5_2114), a nitrogen regulation protein NR(I) gene (BN5_3962) that shares locus with an uncharacterized protein also identified in the table (BN5_3560) and a nitrogen regulation gene (*ntrB*, BN5_3961); a glutaredoxin gene (BN5_4445) located near a FAD-binding oxidoreductase gene (BN5_4444) and a nitrate reductase gene (BN5_4443), a threonylcarbamoyl-AMP synthase gene (BN5_0030) that is closed to an aerobic coproporphyrinogen III oxidase gene (BN5_0032) and the carbamoyl-phosphate synthase small chain gene (BN5_0915), which is near to a dyhydrodipicolinate reductase gene (BN5_0912).

A total of 97 proteins were repressed in the *nitC*$^-$ mutant. Among these proteins were identified the *cbb*$_3$-type cytochrome *c* oxidase subunit and the multidrug resistance protein MdtF (both also repressed in *nitA*$^-$ mutant), together the multidrug resistance protein A (Table 7). In addition, the nitrilase NitC and other three proteins encoded in

the *nit1C* cluster (NitD, NitG and NitH) were found repressed as well as the alpha subunit of the oxaloacetate decarboxylase (W6R3U1). Other proteins repressed in the *nitC*$^{-}$ mutant were a glycerol kinase (W6QUP8), an iron regulated protein A (W6QS54) and serine hydroxymethyltransferase (W6QYM4).

Table 7. Repressed proteins in the *nitC*$^{-}$ mutant strain compared to the wild-type strain under cyanotrophic conditions.

Protein accession number[1]	Gene accession number[2]	*p* -value	F.C.[3]	Description
W6R5U2	BN5_3170	0,002	802,658	GTPase subunit of restriction endonucleas
H9N5E3	BN5_1633	0,000	92,502	Radical SAM domain-containing protein (NitD)
W6R2I8	BN5_2034	0,029	86,087	DNA-binding transcriptional activator OsmE
H9N5D9	BN5_1636	0,000	70,702	Uncharacterized protein (NitG)
W6QXL4	BN5_2662	0,000	63,150	Flagellin
W6R3U1	BN5_4309	0,026	57,940	Oxaloacetate decarboxylase, alpha subunit
W6R0A3	BN5_3590	0,000	40,883	Fatty-acyl-CoA synthase
W6QU73	BN5_1879	0,001	36,765	Putative Anthranilate phosphoribosyltransferase
W6RK11	BN5_3592	0,002	31,554	Acyl-CoA dehydrogenase family protein
W6QTC3	BN5_0616	0,001	28,897	Alpha-2-macroglobulin domain-containing protein
W6R3F4	BN5_2347	0,003	26,520	Cytochrome c550
W6QWP0	BN5_2348	0,000	26,473	PQQ containing dehydrogenase
W6QXF1	BN5_2980	0,010	21,573	OmpA/MotB domain-containing protein
W6RBZ4	BN5_0770	0,018	21,245	Uncharacterized protein
W6QWU6	BN5_0015	0,024	17,223	Glycine--tRNA ligase beta subunit
H9N5D8	BN5_1637	0,002	16,714	FAD dependent oxidoreductase (NitH)
W6REH9	BN5_1658	0,000	16,140	Helix-hairpin-helix repeat-containing competence protein C
W6QS54	BN5_1163	0,011	14,947	Iron-regulated protein A
W6QNX3	BN5_0029	0,013	13,670	DNA protecting protein DprA
W6QWK6	BN5_1792	0,016	12,186	3-oxoacyl-(Acyl-carrier-protein) synthase I
W6QY43	BN5_2354	0,001	12,133	ABC transporter periplasmic protein
W6QY39	BN5_2349	0,000	12,033	Pentapeptide repeat-containing protein
W6QPC7	BN5_0176	0,000	11,925	Mg chelatase, subunit ChlI
W6QXP9	BN5_2187	0,001	11,924	Exonuclease
W6R110	BN5_1506	0,005	11,300	Uncharacterized protein
H9N5E1	BN5_1632	0,000	10,180	Nitrilase (NitC)
W6QZ68	BN5_0862	0,039	10,121	Uncharacterized protein
W6R176	BN5_4266	0,008	9,148	Putative virulence factor
W6QYL6	BN5_3377	0,037	8,120	Uncharacterized protein
W6R8V0	BN5_4267	0,025	7,772	Putative virulence effector protein
W6QWS2	BN5_2737	0,004	7,367	Aminopeptidase N
W6R4D5	BN5_2661	0,000	7,300	Protein flaG
W6RH20	BN5_2649	0,018	7,217	Flagellar assembly protein H
W6QXP8	BN5_3089	0,000	7,197	Aspartyl-tRNA synthetase
W6RGZ5	BN5_2624	0,000	7,028	ParA family protein
W6QYF6	BN5_2952	0,009	6,881	Outer membrane porin
W6QWY4	BN5_2448	0,010	6,621	Cbb3-type cytochrome c oxidase subunit
W6QUJ8	BN5_1565	0,019	6,221	Putative orphan protein
W6R1X7	BN5_4198	0,009	6,200	Laminin subunit gamma-1
W6RDI9	BN5_1328	0,035	6,099	Multidrug resistance protein MdtF
W6QVG9	BN5_1382	0,004	5,526	DNA topoisomerase 1
W6R8B1	BN5_4106	0,000	5,374	Secretion protein HlyD family protein
W6QT42	BN5_1060	0,033	5,308	Phosphoribosylformylglycinamidine synthase
W6R3S5	BN5_4294	0,001	5,232	Uncharacterized protein
W6QV73	BN5_1791	0,004	5,118	Methyl-accepting chemotaxis protein II
W6R8X4	BN5_4292	0,021	4,750	Uncharacterized protein

W6R8X4	BN5_4292	0,021	4,750	Uncharacterized protein
W6QZ57	BN5_3593	0,012	4,473	Beta-lactamase domain-containing protein
W6QXI2	BN5_0237	0,004	4,431	Membrane-fusion protein
W6QWP5	BN5_2353	0,006	4,360	Uncharacterized protein
W6R782	BN5_3669	0,018	4,295	Catalase-peroxidase
W6QVB2	BN5_1327	0,000	3,876	Outer membrane protein OprJ
W6RDK8	BN5_1353	0,024	3,836	Protein CcoG
W6QT23	BN5_0524	0,003	3,797	Protein HflC
W6QUP8	BN5_1116	0,012	3,712	Glycerol kinase
W6RLM7	BN5_4230	0,024	3,700	Integration host factor subunit alpha
W6RDB7	BN5_1247	0,048	3,690	Conserved virulence factor B
W6QVX1	BN5_2456	0,007	3,670	CRP/FNR family transcriptional regulator
W6QSD2	BN5_0279	0,044	3,430	Osmolarity response regulator
W6QZE1	BN5_3663	0,014	3,379	NAD-dependent epimerase/dehydratase
W6QW62	BN5_1647	0,003	3,319	ATP-dependent Clp protease ATP-binding subunit ClpC
W6RHN5	BN5_2779	0,006	3,276	Nitrate reductase
W6R1X9	BN5_1820	0,008	3,264	Methyl-accepting chemotaxis protein McpB
W6QUD7	BN5_1498	0,023	3,260	Alanine--tRNA ligase
W6RE51	BN5_1572	0,015	3,186	Uncharacterized protein
W6QXQ8	BN5_2682	0,006	3,094	Putative flagella synthesis protein FlgN
W6RC60	BN5_0855	0,020	3,003	50S ribosomal protein L21
W6QVW1	BN5_2446	0,017	2,949	Cytochrome c oxidase, cbb3-type, subunit II
W6R591	BN5_2991	0,027	2,908	High-affinity branched-chain amino acid transport ATP-bind
W6QXN9	BN5_2177	0,020	2,894	2-oxoglutarate dehydrogenase, E1 component
W6QZT0	BN5_2953	0,000	2,873	Outer membrane porin F
W6QZM4	BN5_3703	0,005	2,871	DNA-directed RNA polymerase subunit beta
W6QSI2	BN5_0853	0,007	2,859	3-ketoacyl-(Acyl-carrier-protein) reductase
W6QSL8	BN5_1329	0,006	2,721	Multidrug resistance protein A
W6QUY3	BN5_1671	0,024	2,653	Ubiquinone biosynthesis O-methyltransferase
W6QSI1	BN5_0334	0,000	2,652	Methyl-accepting chemotaxis protein I
W6RJG9	BN5_3412	0,028	2,618	Outer membrane protein assembly factor BamD
W6R4T8	BN5_2826	0,011	2,606	Outer membrane protein assembly factor BamA
W6QSQ9	BN5_0930	0,017	2,601	Translation initiation factor IF-2
W6QWJ0	BN5_1772	0,037	2,572	Chaperone protein HtpG
W6RKW1	BN5_3967	0,002	2,441	Chaperone protein ClpB
W6QYM4	BN5_3018	0,032	2,410	Serine hydroxymethyltransferase
W6R2E7	BN5_3881	0,001	2,407	Putative c repressor
W6R197	BN5_3491	0,026	2,368	Bifunctional sulfate adenylyltransferase subunit 1/adenylyl
W6QWF0	BN5_2246	0,032	2,354	Uncharacterized protein
W6R217	BN5_1865	0,034	2,336	Cold shock-like protein CspG
W6QSQ8	BN5_0414	0,012	2,290	Poly(3-hydroxyalkanoate) polymerase
W6R1A2	BN5_3496	0,012	2,279	Histidinol dehydrogenase
W6QWA0	BN5_1657	0,011	2,261	Lipoprotein heavy metal/multidrug efflux protein
W6RHV8	BN5_2834	0,004	2,221	30S ribosomal protein S2
W6QTW8	BN5_1759	0,006	2,213	Universal stress protein E homolog
W6QVI9	BN5_1402	0,027	2,183	Soluble pyridine nucleotide transhydrogenase
W6R3W1	BN5_2507	0,028	2,171	Uncharacterized protein
W6QX80	BN5_2026	0,039	2,155	Sulfite reductase (Ferredoxin)
W6QZ91	BN5_0887	0,017	2,154	OmpA/MotB domain-containing protein
W6QWB9	BN5_1682	0,029	2,063	30S ribosomal protein S1
W6RKF8	BN5_3702	0,008	2,056	DNA-directed RNA polymerase subunit beta'
W6R848	BN5_4039	0,019	2,045	UPF0339 protein in ptx operon 5'region

[1]Accession number from UniProt and [2]Accession number from GenBank (Luque-Almagro *et al.* 2013). [3]Fold Change. Only proteins with a *p*-value ≤ 0.05 and a fold change ≥ 2 were considered

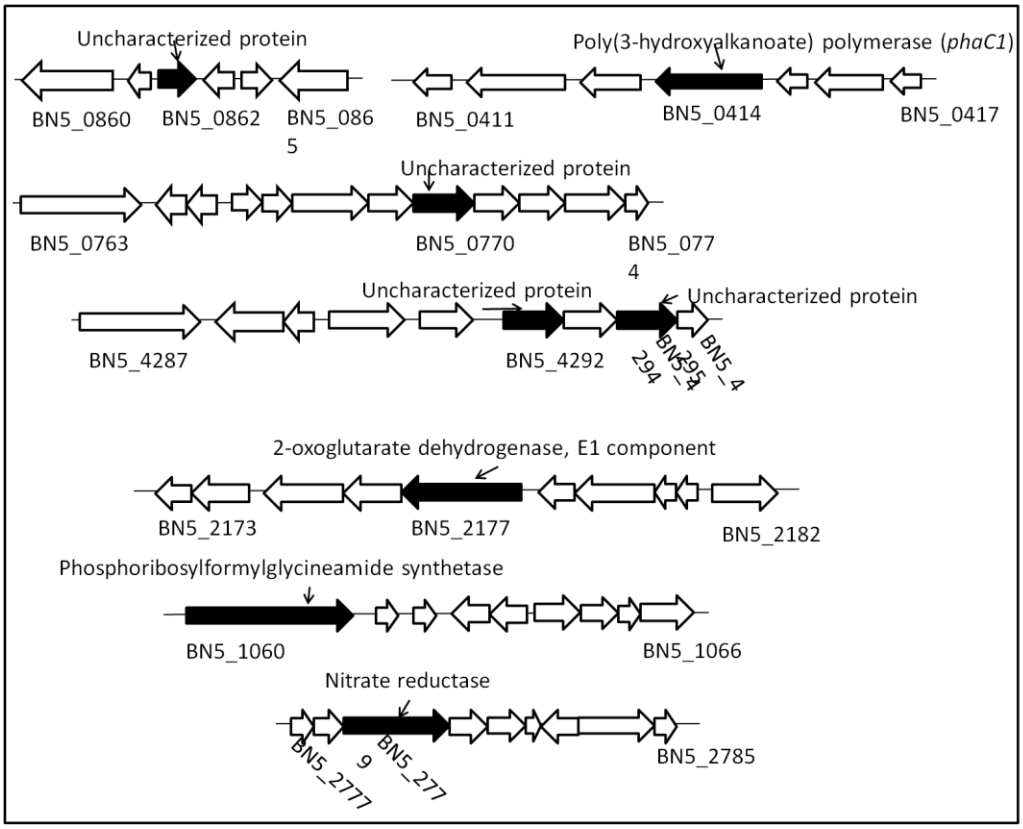

Figure 16. **Gene cluster arrangements with genes that code for proteins specifically repressed in the *nitC*⁻ mutant.** Shown in Table 8.

Some gene cluster encoding proteins repressed in the *nitC*⁻ strain are shown in Figure 16. A poly-3-hydroxyalkanoate polymerase gene (*phaC2*, BN5_0412) clustered together a poly(3-hydroxyalkanoate) depolymerase gene (*phaZ*, BN5_0413) and a TetR family transcriptional regulator *phaD* gene (BN5_0411). Other three proteins have been found repressed in *nitC*⁻ mutant are encoded by the 2-oxoglutarate dehydrogenase gene (BN5_2177), which shares *locus* with the E2 component gene (BN5_2176), the alpha and beta subunits of the succinyl-CoA synthase genes (BN5_2173 and BN5_2174), a dihydropoliamide dehydrogenase gene (BN5_2175), the succinate dehydrogenase genes (BN5_2178, BN5_2179, BN5_2180 and BN5_2181) and the citrate synthase gene (BN5_2182). The phosphoribosylformylglycinamide synthetase gene (BN5_1060) is located near to a phosphoribosylglycinamide formyltransferase gene (BN5_1068) and the nitrate reductase gene (BN5_2779) shares locus with some related genes (*napB,* BN5_2780; *napC,* BN5_2781). Regarding the group of uncharacterized genes, two of

them (BN5_4292 and BN5_4294), form a cluster together three genes related with the CRISPR system (CRISPR-associated helicase Cas3 family, BN5_4287; CRISPR-associated endonuclease Csy4, BN5_4295 and CRISPR-associated protein Csy2, BN5_4293). The gene of an uncharacterized protein (BN5_0770) is located in the same locus than two CRISPR genes that were found induced in the *nitA*$^-$ mutant (Fig. 13). Furthermore, another uncharacterized gene has been found in the same locus than the malate:quinone oxidoreductase (BN5_0860).

The malate:quinone oxidoreductase (W6RC63) and the CbrB regulator (W6RCD4), which were repressed in the *nitA*$^-$ mutant strain (Table 5), were selected to carry out a phylogenetic analysis through the UPGMA method (Sneath and Sokal, 1973) by using homologs from different groups of bacteria (Figs. 17 and 18).

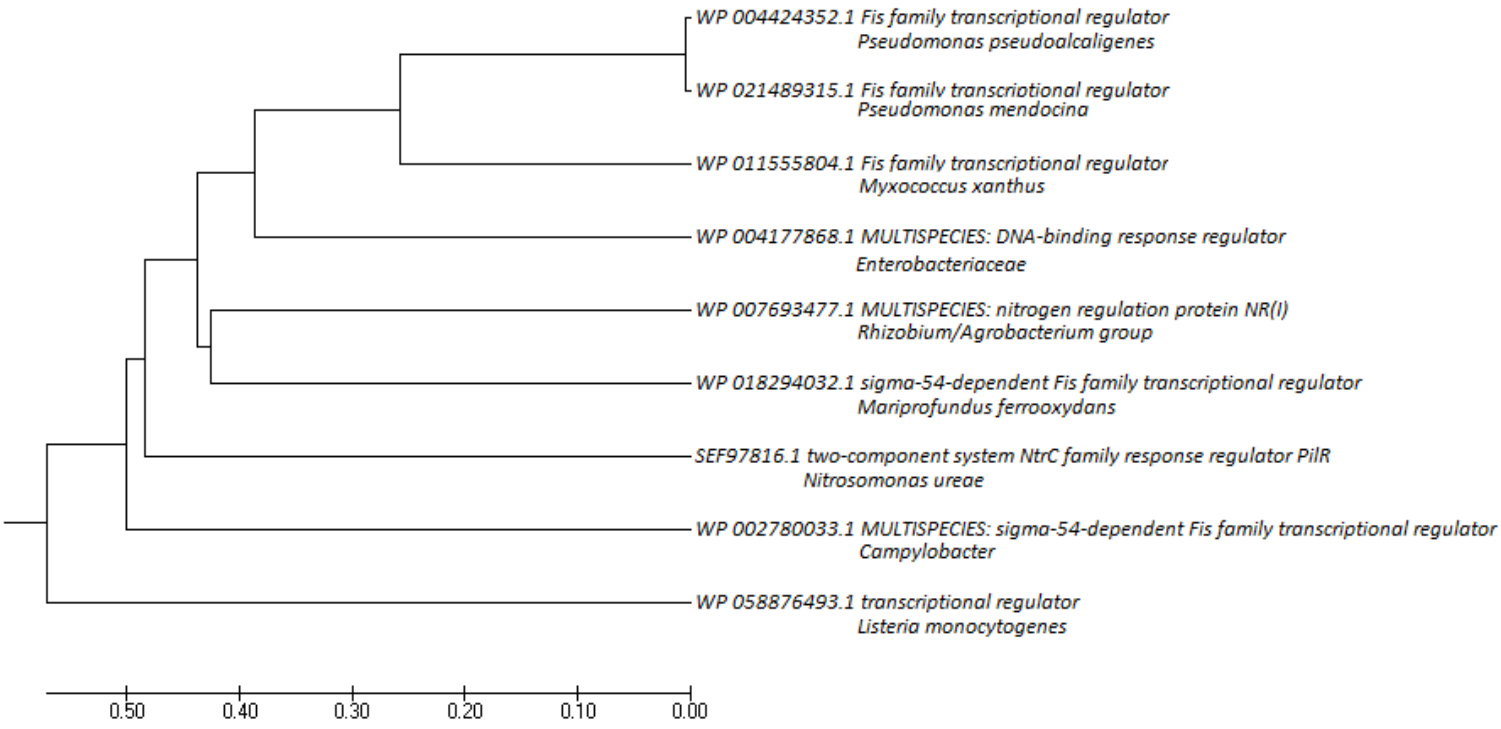

Figure 17. Phylogenetic analysis of the regulatory protein CbrB. The analysis was performed with nine amino acid sequences by using the UPGMA method (Sneath and Sokal, 1973). All positions containing gaps and missing data were eliminated. There were a total of 412 positions in the final dataset.

This analysis showed that the CbrB protein from *P. pseudoalcaligenes* CECT5344 is phylogenetically close to the CbrB protein from *P. mendocina* (Fig. 17). These two proteins, together other gram negative homologs, are grouped and distant from the gram positive bacteria *Listeria*.

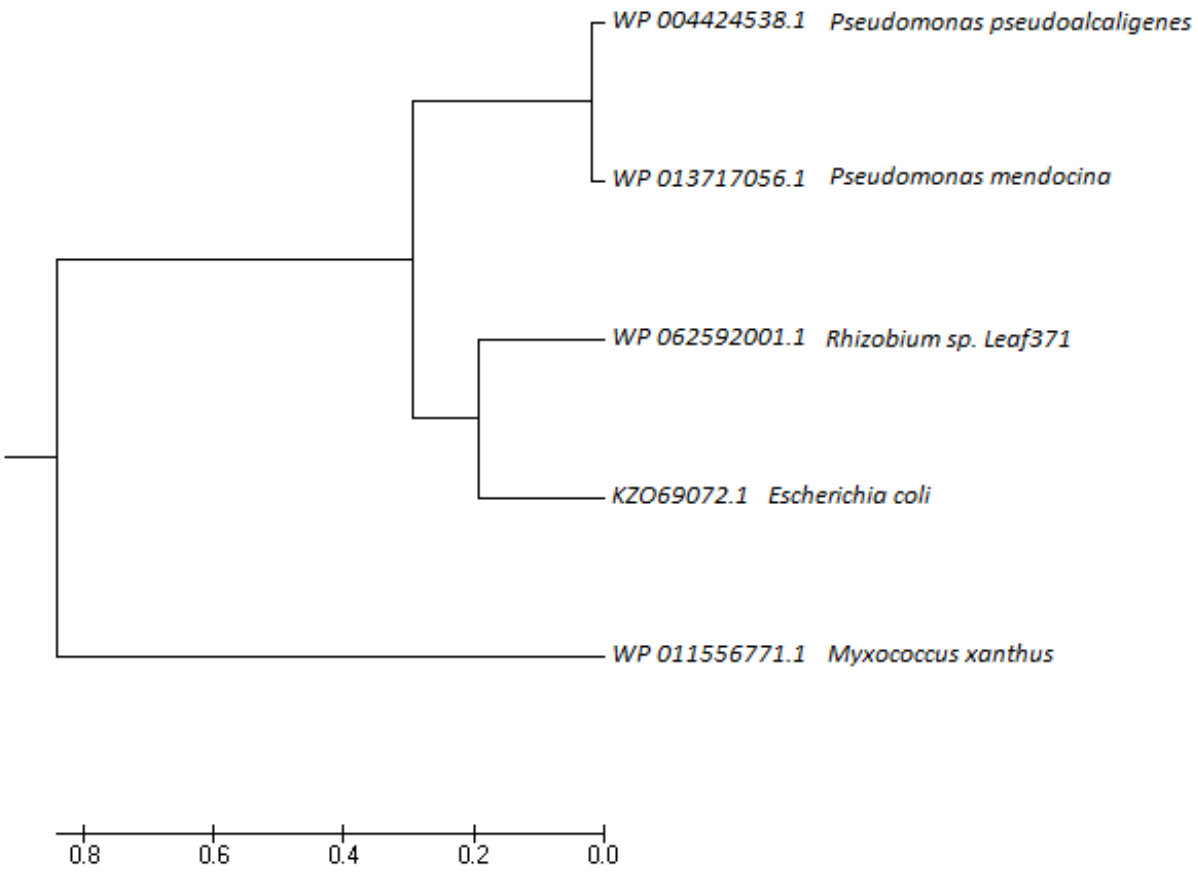

Figure 18. Phylogenetic analysis of the malate:quinone oxidoreductase MqoA. The analysis involved five amino acid sequences. All positions containing gaps and missing data were eliminated. There were a total of 301 positions in the final dataset.

The malate:quinone oxidoreductase phylogenetic analysis (Fig. 18) reveals that the sequence of the malate:quinone oxidoreductase of *P. mendocina* is very similar to the sequence of *P. pseudoalcaligenes* CECT5344, while, *E. coli* is the specie that presents the lowest homology. No homolog sequences have been found in the rest of the species, and in *Myxococcus xanthus* there is homology with an uncharacterized protein.

6. Discussion

Large volumes of cyanide-containing liquid residues are worldwide produced from different industrial activities, highlighting the relevance of efficient techniques to eliminate cyanide from wastewaters. Thus, biological treatments to remove cyanide are proposed (Baxter and Cummings, 2016; Luque-Almagro *et al.*, 2016). The alkaliphilic bacterium *Pseudomonas pseudoalcaligenes* CECT5344 has been described as a cyanotrophic microorganism able to assimilate high concentrations of cyanide (Luque-Almagro *et al.,* 2005). The assimilation of cyanide by the strain CECT5344 occurs *via* oxaloacetate formation, which chemically reacts with cyanide to produce a cyanohydrin or nitrile (Fig. 3). The cyanohydrin of oxaloacetate is converted into its respective carboxylic acid and ammonium by the nitrilase NitC, encoded in the *P. pseudoalcaligenes* CECT5344 *nit1C* gene cluster (Fig. 4). Ammonium is further incorporated to carbon skeletons by the glutamine synthetase/glutamate synthase cycle (Luque-Almagro *et al.*, 2011; Estepa *et al.*, 2012). This cyanide degradation pathway has not been described previously in cyanotrophic microorganisms (Fig. 2). In addition, the whole genome of the strain CECT5344 has been elucidated (Luque-Almagro *et al.*, 2013: Wibberg *et al.*, 2014; Wibberg *et al.,* 2015), which facilitated a transcriptomic study by DNA microarrays of this bacterium in response to cyanide (Luque-Almagro *et al.*, 2015). Recently, a proteomic study by LC-MS/MS of *P. pseudoalcaligenes* CECT5344 in response to cyanide has been also carried out (Ibañez *et al*., unpublished).

In this work, the BN-PAGE technique has been applied to identify soluble protein complexes that could have a role in cyanide detoxification/assimilation in *P. pseudoalcaligenes* CECT5344. Two protein complexes have been identified (Fig. 6, Table 3) as complex I, which is composed of the phosphoenolpyruvate synthase (W6QUW7) and the chaperone DnaK (W6RCA2), and complex II formed by the phosphoenolpyruvate carboxylase (W6Q792) and the subunit B of the pyruvate carboxylase (W6R3U1). Phosphoenolpyruvate synthase phosphorilates pyruvate to produce phosphoenolpyruvate, Phosphoenolpyruvate carboxylase produces oxaloacetate from phosphoenolpyruvate and pyruvate carboxylase catalyzes the conversion of pyruvate into oxaloacetate (Cooper and Kornberg, 1967; Mathews *et al.,* 2003; Shane *et al.,* 2013). The phosphoenolpyruvate synthase shows protein interactions with pyruvate carboxyalse (oxaloacetate decarboxylase) (Fig. 10). These enzymes, organized in two

protein complexes, might work together to produce oxaloacetate in response to cyanide in *P. pseudoalcaligenes* CECT5344, which constitutes the first step in cyanide assimilation in this bacterium (Estepa et al., 2012). Furthermore, not only oxaloacetate but also pyruvate, react with cyanide to produce cyanohydrins, and both cyanohydrins have been previously demonstrate that can be used as nitrogen source by the strain CECT5344 (Luque-Almagro *et al.*, 2011; Estepa *et al.*, 2012). Although all three enzymes were induced by cyanide, they are key enzymes in carbon metabolism, independently on the nitrogen source used by bacteria. However, these enzymes were not detected by BN-PAGE carried out with soluble fractions from cells grown with ammonium, probably because they are found at concentrations below the detection limit of this technique.

The *dnaK* gene cluster includes another gene that codes for the dihydropicolinate reductase DapB (Fig. 8). The dihydropicolinate reductase catalyzes the second step of lysine biosynthesis, producing 2,3,4,5-tetrahydropicolinic acid from dipicolinic acid (Fig. 9) (Paiva *et al.* 2001; Girish *et al.,* 2011; Escribano, 2016). The *dapA* gene (BN5_ 0911) has been found induced by cyanide in the transcriptomic analysis carried out in the CECT5344 strain (Luque-Almagro *et al.*, 2015), but its role in cyanide degradation has not been elucidated yet. In addition, the dihydropicolinate synthase DapA (W6R260) has been also found induced by cyanide in the BN-PAGE analysis performed in this work as protein (Fig. S1 and Table S1). The product of the dihydropicolinate synthase DapA is the dihydropicolinic acid, which has been described to function as iron chelator with a possible role in iron storage, and therefore, in recycling iron-sulfur clusters in metalloenzymes that could be damaged by cyanide (Maringanti and Imlay, 1999; Escribano, 2016).

The *P. pseudoalcaligenes* CECT5344 *nit1C* cluster has been demonstrated to be essential for cyanide assimilation. Thus, a nitrilase defective mutant *nitC*$^{-}$ and a transcriptional regulator defective mutant *nitA*$^{-}$ of *P. pseudoalcaligenes* CECT5344 were previously generated and their inability to grow with cyanide established (Estepa *et al.*, 2012). Similar results have been found in a mutant strain JL102 of *Pseudomonas fluorescens* NCIMB 11764, unable to grow with cyanide because it lacks of cyanide-degrading enzyme (Kunz *et al.,* 1998). Before carrying out the proteomic analysis of the *nitA*$^{-}$ and

nitC$^-$ mutants a further characterization of these strains in cyanide-containing media has been performed. The *nitA*$^-$ and *nitC*$^-$ mutants were unable to growth with cyanide (Fig. 11), as previously demonstrated, and were deficient in the cyanide-inducible nitrilase NitC activity when compared to the wild-type strain (Fig. 12). Although these results corroborate that none of the three additional nitrilases of *P. pseudoalcaligenes* CECT5344 participate in cyanide assimilation, they may have a role in cyanide detoxification.

The global proteomic characterization of the *nitA*$^-$ and *nitC*$^-$ mutants of *P. pseudoalcaligenes* CECT5344 has been performed by using the LC-MS/MS technique. The *nitA*$^-$ mutant showed induced proteins (Table 4), such as the isochorismate hydrolase (W6RI94) involved in nicotininamide and nicotinate metabolism, the phasin-like protein PhaP (W6R8A0), two CRISPR/Cas-associated proteins (W6QR33 and W6QZ01) and the glutathione peroxidase (W6RC90). The inability of the *nitA*$^-$ mutant strain to use cyanide as nitrogen source probably causes an induction of the CRISPR system, which is a prokaryotic immune system that confers protection to bacteria against plasmids and phages (Barrangou *et al.,* 2007). This may suggest that in presence of cyanide, the CRISPR system is repressed in the wild-type strain, probably to allow exogenous DNA to enter into the cell, increasing the possibilities of the bacterium to survive on cyanide. The *nitA*$^-$ mutant also contains in its proteome repressed proteins (Table 5), such as proteins belonging to the Nit1C system (NitC, NitB, NitD, NitH, and NitG), which are not required in this mutant strain because cyanide is not assimilated. The isocitrate lyase (W6REY3), a metal extrusion protein (W6QSL8), the malate:quinone oxidoreductase MqoA (W6RC63), the regulatory protein CbrB (W6RCD4) and the cbb_3-type oxidase (W6VW1) were also repressed. In the transcriptomic and proteomic studies previously carried out in the wild-type strain of *P. pseudoalcaligenes* CECT5344, a common response to cyanide was the induction of enzymes with cofactors (with either metal or organic nature), such as PLP-enzymes and haemproteins, and also the repression of the CRISPR/Cas-associated proteins. The malate:quinone oxidoreductase (MqoA) provides with electrons the cyanide-insensitive terminal oxidase (CioAB) by

converting L-malate into oxaloacetate, and therefore Mqo is a key enzyme in the first step of cyanide degradation in *P. pseudoalcaligenes* CECT5344 since this bacterium lacks malate dehydrogenase (Luque-Almagro *et al.*, 2011). Although *P. pseudoalcaligenes* CECT5344 presents two malate:quinone oxidoreductases (MqoA and MqoB), only one of them, the MqoA (W6RC63), which is also present in other bacteria (Fig. 18), was repressed in the *nitA*$^-$ mutant, probably because in the absence of cyanide its activity may be reduced for a lower requirement of electron to the electron transport chain. The regulatory protein CbrB (W6RCD4) belongs to a two-component regulatory system, being the response component. The CbrAB system is involved in regulation of catabolism of different amino acid, responding to the C/N ratio in the cell. In *Pseudomonas aeruginosa* these amino acids usually are arginine, ornitine, putresceine, among others (Nishijyo *et al*., 2001). In *P. pseudoalcaligenes* CECT5344, the CrbAB system may have a role in amino acid catabolism associated to cyanide assimilation because from the previous transcriptomic and proteomic data a relationship between different amino acids and cyanide metabolism could be established (Luque-Almagro *et al.*, 2015; Ibañez *et al.*, unpublished). Additionally, the CbrAB system, which is widespread among bacteria (Fig. 17), may play a more general role related with the C/N balance.

Concerning the proteome of the *nitC*$^-$ mutant of *P. pseudoalcaligenes* CECT5344, some induced proteins (Table 6) were related to carbon metabolism, like the fumarate hydratase (W6RE08), whereas other proteins were related to nitrogen starvation, like the global nitrogen response regulator NtrC (W6RKV8), the urease components (W6QYG3 and W6RBC9) and the periplasmic nitrate transporter (W6QUU3). Also, proteins involved in general stress response like glutaredoxin (W6RM46), glutathione peroxidase (W6RC90) and alkyl hydroperoxide reductase (W6R9C0) were induced by cyanide. Additionally, proteins related to methionine and *S*-adenosylmethionine (SAM) were also induced *nitC*$^-$ mutant, such as homoserine kinase (W6QRT8) and *S*-adenosylmethionine synthase (W6RAS5). The fumarate hydratase (fumarase) convers fumarate into L-malate, which is the substrate of the malate:quinone oxidoreductase. Furthermore, there are two types of fumarases; class I fumarases have Fe^{2+} as cofactor, whereas class II fumarases are devoided of cofactor. It has been described that cyanide

has a strong affinity for metal, causing inhibition of metalenzymes. Probably, in the presence of high concentrations of cyanide the class II fumarase is induced due to its resistance to cyanide and, probably to compensate the inactivation caused by cyanide of the fumarase clas I in the CECT5344 strain. The induction of proteins related with nitrogen starvation can be directly associated with the inability of the *nitC*$^{-}$ mutant strain to assimilate cyanide. This response to nitrogen starvation has been also observed in the transcriptomic study when *P. pseudoalcaligenes* CECT5344 cells were subjected to nitrogen limiting conditions (Luque-Almagro *et al.,* 2007; Luque-Almagro *et al.*, 2015). The induction of methionine and SAM-related enzymes could be explained by the existence of a radical SAM-containing protein, which is encoded in the *nit1C* gene cluster of the strain CECT5344 and could be required for cyanide assimilation. In the *nitC*$^{-}$ mutant, cyanide provokes an oxidative stress response higher than in the wild-type strain because in this mutant strain cyanide cannot be assimilated. The enzymes hydroperoxide reductase and glutathione peroxidase are involved in the oxidative stress response (Nallabelli *et al.,* 2016). Glutathione provides defense against oxidative stress by eliminating free radicals or by participating in the reduction of hydroperoxide (Hayes and Mclellan, 1999) Glutaredoxin acts as an antioxidant mechanism by reducing dehydroascorbate and peroxiredoxins. In addition, glutaredoxin binds to iron-sulfur clusters, contributing to their delivery to enzymes (Rouhier *et al.,* 2008).

On the other hand, proteins repressed in the the *nitC*$^{-}$ mutant of *P. pseudoalcaligenes* CECT5344 (Table 7) were, as previously described in the *nitA*$^{-}$ proteome, proteins belonging to the Nit1C system involved in cyanide assimilation (NitC, NitD, NitH, and NitG), which are not required in this mutant strain because cyanide is not assimilated, as well as a metal extrusion protein (W6QSL8) and the cbb_3-type oxidase (W6VW1). Specifically repressed proteins in the *nitC*$^{-}$ mutant were oxaloacetate decarboxylase (pyruvate carboxylase, W6R3U1), which was induced by cyanide and was identified by the BN-PAGE technique as part of complex II, glycerol kinase (W6QUP8), a poly(3-hydroxyalkanoate) polymerase (W6QSQ8) and a phosphoribosylglycinamide synthase (W6QT42). Another phosphoribosylglycinamide formyltransferase (NitF) is encoded in the *nit1C* gene cluster of the strain CECT5344 and could have a role in cyanide

assimilation, although its activity is usually related with *de novo* synthesis of purines (Connelly *et al.* 2013).

7. Conclusions:

The main conclusions derived from this work are the following:

1. Two protein complexes induced by cyanide in *P. pseudoalcaligenes* CECT5344 have been identified by BN-PAGE. These complexes can be involved in the synthesis of oxaloacetate required for cyanide assimilation.
2. The mutant strains *nitA*$^-$ and *nitC*$^-$ of *P. pseudoalcaligenes* CECT5344, which are unable to grow with cyanide, have been characterized by LC-MS/MS. Both mutant strains induced proteins encoded by the *nit1C* gene cluster that is essential for cyanide assimilation in this bacterium. Specifically, the *nitA*$^-$ mutant induced CRISPR/Cas associated proteins related with exogenous DNA capitation, whereas the malate:quinone oxidoreductase MqoA was repressed. The *nitC*$^-$ mutant strain of *P. pseudoalcaligenes* CECT5344 specifically induced proteins related to nitrogen starvation and oxidative stress, while proteins related to carbon metabolism were repressed.

8. References:

Acheampong, M. A., Meulepas, R. J. and Lens, P. N. (2010). Removal of heavy metals and cyanide from gold mine wastewater. *Journal of Chemical Technology and Biotechnology*, 85, 590-613.

Asmus, E., and Garschagen, H. (1953). The use of barbituric acid for the photometric determination of cyanide and thiocyanate. *Zeitschrift für Analytical Chemistry*, 138, 414-422.

Barrangou, R., Fremaux, C., Deveau, H., Richards, M., Boyaval, P., Moineau, S., Romero A., D. and Horvath, P. (2007). CRISPR provides acquired resistance against viruses in prokaryotes. *Science*, 315, 1709-1712.

Baxter, J., and Cummings, S. P. (2006). The current and future applications of microorganism in the bioremediation of cyanide contamination. *Antonie Van Leeuwenhoek*, 90, 1-17.

Blumer, C. and Haas, D. (2000). Mechanism, regulation, and ecological role of bacterial cyanide biosynthesis. *Archives of Microbiology*, 173, 170-177.

Boening, D. W. and Chew, C. M. (1999). A critical review: general toxicity and environmental fate of three aqueous cyanide ions and associated ligands. *Water, Air, and Soil Pollution*, 109, 67-79.

Bradford, M. M. (1976). A rapid and sensitive method for the quantitation of microgram quantities of protein utilizing the principle of protein-dye binding. *Analytical Biochemistry*, 72, 248-254.

Bucca, G., Brassington, A. M., Hotchkiss, G., Mersinias, V. and Smith, C. P. (2003). Negative feedback regulation of *dnaK*, *clpB* and ion expression by the DnaK chaperone machine in *Streptomyces coelicolor*, identified by transcriptome and in vivo DnaK-depletion analysis. *Molecular Microbiology*, 50, 153-166.

Connelly, S., DeMartino, J. K., Boger, D. L. and Wilson, I. A. (2013). Biological and structural evaluation of 10 R-and 10 S-methylthio-DDACTHF reveals a new role for sulfur in inhibition of glycinamide ribonucleotide transformylase. *Biochemistry*, 52, 5133-5144.

Cooper, R. A., and Kornberg, H. L. (1967). The mechanism of the phosphoenolpyruvate synthase reaction. *Biochimica et Biophysica Acta (BBA)-General Subjects*, 141, 211-213.

Dash, R. R., Gaur, A. and Balomajumder, C. (2009). Cyanide in industrial wastewaters and its removal: A review on biotreatment. *Journal of Hazardous Materials*, 163, 1-11.

Ebbs, S. (2004). Biological degradation of cyanide compounds. *Current Opinion in Biotechnology*, 15, 231-236.

Escribano, M., P. (2016). Análisis transcriptómico y proteómico de *Pseudomonas pseudoalcaligenes* CECT5344 en respuesta a cianuro. Tesis doctoral, Universidad de Córdoba, UCOPress.

Estepa, J., Luque-Almagro, V. M., Manso, I., Escribano, M. P., Martínez-Luque, M., Castillo, F., Moreno-Vivián, C. and Roldán, M. D. (2012). The *nit1C* gene cluster of *Pseudomonas pseudoalcaligenes* CECT5344 involved in assimilation of nitriles is essential for growth on cyanide. *Environmental Microbiology Reports*, 4, 326-334.

Fiala, G. J., Schamel, W. W., and Blumenthal, B. (2011). Blue native polyacrylamide gel electrophoresis (BN-PAGE) for analysis of multiprotein complexes from cellular lysates. *JoVE (Journal of Visualized Experiments)*, 48, 2164.

Girish, T. S., Navratna, V., & Gopal, B. (2011). Structure and nucleotide specificity of *Staphylococcus aureus* dihydrodipicolinate reductase (DapB). *FEBS letters*, 585, 2561-2567.

Hayes, J. D., and Mclellan, L. I. (1999). Glutathione and glutathione-dependent enzymes represent a co-ordinately regulated defence against oxidative stress. *Free Radical Research*, 31, 273-300.

Kai, Y., Matsumura, H. and Izui, K. (2003). Phosphoenolpyruvate carboxylase: three-dimensional structure and molecular mechanisms. *Archives of Biochemistry and Biophysics*, *414*(2), 170-179.

Kanehisa, M., Sato, Y., Kawashima, M., Furumichi, M., and Tanabe, M. (2016), KEGG as a reference resource for gene and protein annotation. Nucleic Acids Research. 44, D457-D462.

Kumar S, Stecher G, and Tamura K (2016) MEGA7: Molecular Evolutionary Genetics Analysis version 7.0 for bigger datasets. *Molecular Biology and Evolution* 33:1870-1874.

Kunz, D. A., Chen, J. L., and Pan, G. (1998). Accumulation of α-keto acids as essential components in cyanide assimilation by *Pseudomonas fluorescens* NCIMB 11764. *Applied and Environmental Microbiology*, 64, 4452-4459.

Kuyucak, N. and Akcil, A. (2013). Cyanide and removal options from effluents in gold mining and metallurgical processes. *Minerals Engineering*, 50, 13-29.

Li, H., Li, B., Jin, L. Y., Kan, Y. and Yin, B. (2011). A rapid responsive and highly selective probe for cyanide in the aqueous environment. *Tetrahedron*, 67, 7348-7353.

Logsdon, M. J., Hagelstein, K. and Mudder, T. (1999). The management of cyanide in gold extraction. International Council on Metals and the Environment, *International Council on Metals and the Environment Publications,* Canada Ottawa.

Luque-Almagro, V. M., Blasco, R., Huertas, M. J., Martínez-Luque, M., Moreno-Vivián, C., Castillo, F. and Roldán, M. D. (2005). Alkaline cyanide biodegradation by *Pseudomonas pseudoalcaligenes* CECT5344. *Biochemical Society Transactions*, 33, 168-169.

Luque-Almagro, V. M., Huertas, M. J., Roldán, M. D., Moreno-Vivián, C., Martínez-Luque, M., Blasco, R., and Castillo, F. (2007). The cyanotrophic bacterium Pseudomonas pseudoalcaligenes CECT5344 responds to cyanide by defence mechanisms against iron deprivation, oxidative damage and nitrogen stress. *Environmental Microbiology*, 9, 1541-1549.

Luque-Almagro, V. M., Merchan, F., Blasco, R., Igeño, M. I., Martínez-Luque, M., Moreno-Vivian, C., Castillo, F. and Roldán, M. D. (2011). Cyanide degradation by *Pseudomonas pseudoalcaligenes* CECT5344 involves a malate:quinone oxidoreductase and an associated cyanide-insensitive electron transfer chain. *Microbiology*, 157, 739-746.

Luque-Almagro, V. M., Acera, F., Igeño, M. I., Wibberg, D., Roldán, M. D., Sáez, L. P., Hennig, M., Quesada, A., Huertas, M. J., Blom, J., Merchán, F., Escribano, M. P., Jaenicke, S., Estepa, J., Guijo, M. I., Martínez-Luque, M., Macías, D., Szczepanowski, R., Becerra, G., Ramirez, S., Carmona, M. I., Gutiérrez, O., Manso, I., Pühler, A., Castillo, F., Moreno-Vivián, C., Schlüter, A. and Blasco, R. (2013). Draft whole genome sequence of the cyanide-degrading bacterium *Pseudomonas pseudoalcaligenes* CECT5344. *Environmental Microbiology*, 15, 253-270.

Luque-Almagro, V. M., Escribano, M. P., Manso, I., Sáez, L. P., Cabello, P., Moreno-Vivián, C., & Roldán, M. D. (2015). DNA microarray analysis of the cyanotroph *Pseudomonas pseudoalcaligenes* CECT5344 in response to nitrogen starvation, cyanide and a jewelry wastewater. *Journal of Biotechnology*, 214, 171-181.

Luque-Almagro, V. M., Moreno-Vivián, C. and Roldán, M. D. (2016). Biodegradation of cyanide wastes from mining and jewellery industries. *Current Opinion in Biotechnology*, 38, 9-13.

Maniatis, T., Fritsch, E. F., and Sambrook J. (1982) Molecular Cloning: A Laboratory Manual. *CSH Laboratory, Cold Spring Harbor, NY*, 368-369.

Manso. I., Ibañez, M. I., Peña, F., Sáez, L. P., Luque-Almagro, V. M., Castillo, F., Roldán, M. D., Prieto, M. A., Moreno-Vivián, C. (2015). *Pseudomonas pseudoalcaligenes* CECT5344, a cyanide-degrading bacterium with by-product (polyhydroxyalkanoates) formation capacity. *Microbial Cell Factories*, 14, 1.

Maringanti, S. and Imlay, J. A. (1999). An Intracellular Iron Chelator Pleiotropically Suppresses Enzymatic and Growth Defects of Superoxide Dismutase-Deficient *Escherichia coli*. *Journal of Bacteriology*, 181, 3792-3802.

Mathews, C. K.; Van Holde, K.E; Ahern, K.G (2003). *Biochemistry.* 3ª ed. St. Francisco. Pearson Education.

Matthews, C. N., and Minard, R. D. (2006). Hydrogen cyanide polymers, comets and the origin of life. *Faraday Discussions*, 133, 393-401.

Matzke, M. M., Brown, J. N., Gritsenko, M. A., Metz, T. O., Pounds, J. G., Rodland, K. D., Shukla, A. K., Smith, R. D., Waters, K. M., McDemott, J. E. and Webb-Robertson, B. J. (2013). A comparative analysis of computational approaches to relative protein quantification using peptide peak intensities in label-free LC-MS proteomics experiments. *Proteomics*, 13, 493-503.

Michaels, R. and Corpe, W. A. (1965). Cyanide formation by *Chromobacterium violaceum*. *Journal of Bacteriology*, 89, 106-112.

Mirizadeh, S., Yaghmaei, S. and Nejad, Z. G. (2014). Biodegradation of cyanide by a new isolated strain under alkaline conditions and optimization by response surface methodology (RSM). *Journal of Environmental Health Science and Engineering*, 12, 1.

Morrison, G. R. (1971). Microchemical determination of organic nitrogen with Nessler reagent. *Analytical Biochemistry*, 43, 527-532.

Nallabelli, N., Patil, P. P., Pal, V. K., Singh, N., Jain, A., Patil, P. B., Grover. V.and Korpole, S. (2016). Biochemical and genome sequence analyses of *Megasphaera sp*. strain DISK18 from dental plaque of a healthy individual reveals commensal lifestyle. *Scientific Reports*, 6.

Nishijyo, T., Haas, D., and Itoh, Y. (2001). The CbrA–CbrB two-component regulatory system controls the utilization of multiple carbon and nitrogen sources in *Pseudomonas aeruginosa*. *Molecular Microbiology*, 40, 917-931.

Nishino, K., and Yamaguchi, A. (2001). Analysis of a complete library of putative drug transporter genes in *Escherichia coli*. *Journal of Bacteriology*, 183, 5803-5812.

Paiva, A. M., Vanderwall, D. E., Blanchard, J. S., Kozarich, J. W., Williamson, J. M. and Kelly, T. M. (2001). Inhibitors of dihydrodipicolinate reductase, a key enzyme of the diaminopimelate pathway of *Mycobacterium tuberculosis*. *Biochimica et Biophysica Acta (BBA)-Protein Structure and Molecular Enzymology*, 1545, 67-77.

Pötter, M., Madkour, M. H., Mayer, F., and steinbüchel, A. (2002). Regulation of phasin expression and polyhydroxyalkanoate (PHA) granule formation in *Ralstonia eutropha* H16. *Microbiology*, 148, 2413-2426.

Quesada, A., Guijo, M. I., Merchán, F., Blázquez, B., Igeño, M. I. and Blasco, R. (2007). Essential role of cytochrome bd-related oxidase in cyanide resistance of Pseudomonas pseudoalcaligenes CECT5344. *Applied and Environmental Microbiology*, *73*, 5118-5124.

Raybuck, S. A. (1992). Microbes and microbial enzymes for cyanide degradation. *Biodegradation*, 3, 3-18.

Reisinger, V. and Eichacker, L. A. (2008). Solubilization of membrane protein complexes for blue native PAGE. *Journal of Proteomics*, 71, 277-283.

Rouhier, N., Lemaire, S. D., and Jacquot, J. P. (2008). The role of glutathione in photosynthetic organisms: emerging functions for glutaredoxins and glutathionylation. *Annual Review. Plant Biology*, 59, 143-166.

Sarma, D. S. R., Rajalakshmi, S. and Sarma, P. S. (1964). Studies of the enzymes involved in nicotinamide adenine dinucleotide metabolism in *Aspergillus niger. Biochimica et Biophysica Acta (BBA)-Specialized Section on Enzymological Subjects*, 81, 311-322.

Shakir, F. K., Audilet, D., Drake, A. J. and Shakir, K. M. (1994). A rapid protein determination by modification of the Lowry procedure. *Analytical Biochemistry*, 216, 232.

Shane, M. W., Fedosejevs, E. T., and Plaxton, W. C. (2013). Reciprocal control of anaplerotic phosphoenolpyruvate carboxylase by in vivo monoubiquitination and phosphorylation in developing protenoid roots of phosphate-deficient harsh hakea. *Plant Physiology*, 161, 1634-1644.

Sneath, P. H. and Sokal, R. R. (1973). Numerical taxonomy. The principles and practices of numerical classification. *WF Freeman and Company., San Francisco*, *573*.

Solorzano, L. (1969). Determination of ammonia in natural waters by the phenolhypochlorite method. *Limnology and Oceanography*, 14, 799-801.

Sutherland, J. D. (2016). The origin of life—out of the blue. *Angewandte Chemie International Edition*, 55, 104-121.

Szklarczyk D, Franceschini A, Wyder S, Forslund K, Heller D, Huerta-Cepas J, Simonovic M, Roth A, Santos A, Tsafou KP, Kuhn M, Bork P, Jensen LJ, von Mering C. (2015), STRING v10: protein-protein interaction networks, integrated over the tree of life. *Nucleic Acids Reserch*, 43:D44752.

Wibberg, D., Luque-Almagro, V. M., Igeño, M. I., Bremges, A., Roldán, M. D., Merchán, Sáez L. P., Guijo, M. I., Manso, M. I., Macías D., F., Cabello, P., Becerra, G., Ibáñez M. I., Carmona, M. I., Escribano M. P., Castillo, F., Sczyrba, A., Moreno-Vivián, C., Blasco, R., Pühler, A., and Schlüter, A. (2014). Complete genome sequence of the cyanide-degrading bacterium *Pseudomonas pseudoalcaligenes* CECT5344. *Journal of Biotechnology*, *175*, 67-68.

Wibberg, D., Bremges, A., Dammann-Kalinowski, T., Maus, I., Igeño, M. I., Vogelsang, R., König, C., Luque-Almagro, V. M., Roldán M. D., Sczyrba, A., Moreno-Vivián, C., Blasco, R., Pühler, A. and Schlüter, A. (2016). Finished genome sequence and methylome of the cyanide-degrading *Pseudomonas pseudoalcaligenes* strain CECT5344 as resolved by single-molecule real-time sequencing. *Journal of Biotechnology* 232, 61-68.

Wittig, I., Braun, H. P., and Schägger, H. (2006). Blue native PAGE. *Nature Protocols*, 1, 418-428.

Xu, Z., Chen, X., Kim, H. N. and Yoon, J. (2010). Sensors for the optical detection of cyanide ion. *Chemical Society Reviews*, 39, 127-137.

10. Supplementary Material

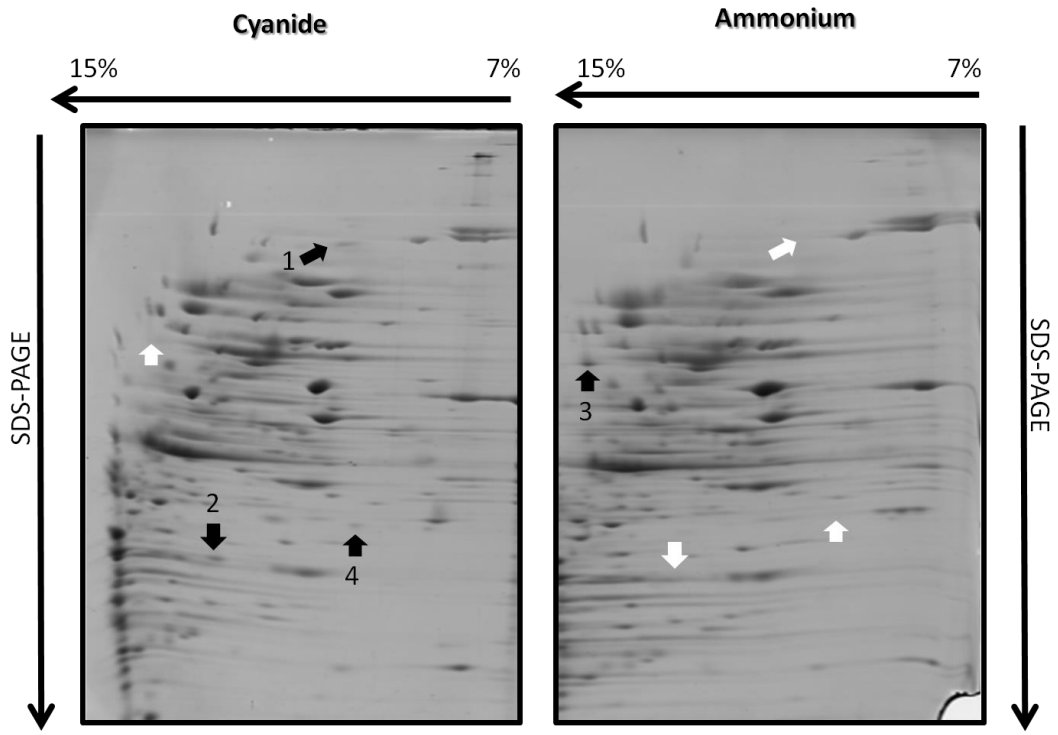

Figure S1. Unaligned proteins induced and repressed by sodium cyanide. The black arrows indicate the presence of a spot, while the white arrows determine the absence of spot. Spots 1, 2 and 3 are induced by cyanide and spot 3 is repressed by cyanide.

Table S1. Unaligned proteins identified by BN-PAGE. Among others, the molecular weight, the accession number, the score of the protein are represented.

Spot Nº	Protein name	Accesion number *	Score C.I. %	Score	P.I.	Molecular Weight (Da)
1	Beta-alanine--pyruvate transaminase	W6QZ51	100	122	6.4	48720.6
2	Dihydrodipicolinate synthase	W6R260	100	248	5.36	33877.4
3	Cooper oxidase	W6QVS6	100	651	5.77	67465.6
4	Succinyl-CoA ligase [ADP-forming] subunit alpha	W6QV49	100	509	5.78	30495.7

(*) Accession number according to the UniProt Consortium, (2014)

Table S2. Comparative analysis of *nitA*⁻ and *nitC*⁻ mutants. Induced proteins in *nitC*⁻ mutant.

Protein accession number[1]	Gene accession number[2]	*p* -value	F.C.[3]	Description
W6QZP2	BN5_3732	0,002	19,127	N-acetyl-gamma-glutamyl-phosphate reductase
H9N5E3	BN5_1633	0,040	16,357	Radical SAM domain-containing protein
H9N5E2	BN5_1631	0,000	13,209	Uncharacterized protein
W6QS37	BN5_0708	0,006	9,014	Uncharacterized protein
W6QUU3	BN5_2114	0,015	7,711	Nitrate transporter periplasmic component
W6QVZ5	BN5_2095	0,041	7,382	Outer membrane porin, OprD family
W6QST4	BN5_0439	0,001	6,818	ABC-type transporter periplasmic component protein
W6RAC3	BN5_0149	0,022	6,777	Putative endoribonuclease L-PSP
W6R184	BN5_3476	0,005	6,762	Transport-associated
W6RKV8	BN5_3962	0,014	6,497	Nitrogen regulation protein NR(I)
W6RJD4	BN5_3371	0,043	6,322	Ribose-phosphate pyrophosphokinase
W6R1T8	BN5_4163	0,036	6,283	Putative aliphatic sulfonates-binding protein
W6QX60	BN5_2518	0,011	6,133	Metallo-beta-lactamase family protein
W6QXC5	BN5_0151	0,014	6,023	Flavin monoamine oxidase-related protein
W6QVB9	BN5_2244	0,018	5,863	Transglutaminase domain-containing protein
W6RBC9	BN5_0552	0,009	5,598	Urease accessory protein UreG
W6QQX9	BN5_0308	0,024	5,489	Glutathione synthetase
W6R0B8	BN5_3142	0,017	5,468	Peptidyl-prolyl cis-trans isomerase
W6R1S2	BN5_1750	0,022	5,130	ATP-dependent Clp protease ATP-binding subunit ClpX
W6QYX9	BN5_0737	0,020	5,071	Peptidase U62, modulator of DNA gyrase
W6QYX2	BN5_0727	0,035	4,849	Aspartyl/glutamyl-tRNA(Asn/Gln) amidotransferase subunit B
W6RBR8	BN5_0665	0,001	4,836	Fimbrillin
W6QTI9	BN5_0646	0,005	4,641	Serine hydroxymethyltransferase
W6R1A4	BN5_3960	0,013	4,171	Uncharacterized protein
W6QSY1	BN5_0484	0,019	3,923	Bifunctional protein HldE
W6QYV0	BN5_3096	0,005	3,791	Porin D
W6QXB4	BN5_2061	0,029	3,787	UTP--glucose-1-phosphate uridylyltransferase
W6R3I5	BN5_2387	0,010	3,769	3-isopropylmalate dehydratase small subunit
W6QPU0	BN5_0346	0,040	3,761	Phosphoglycerate kinase
W6RJH5	BN5_3422	0,000	3,753	Putative Tfp pilus assembly protein
W6QTN7	BN5_1245	0,030	3,518	Soluble aldose sugar dehydrogenase yliI
W6QZH3	BN5_2843	0,003	3,484	Amino acid ABC transporter periplasmic protein
W6QPA6	BN5_0150	0,026	3,465	Cytochrome C6
W6RJS0	BN5_3512	0,024	3,450	PTS IIA-like nitrogen-regulatory protein PtsN
W6RB01	BN5_0425	0,024	3,449	Malate dehydrogenase (Oxaloacetate-decarboxylating)
W6RAS5	BN5_0340	0,016	3,363	S-adenosylmethionine synthase
W6RFX0	BN5_2178	0,016	3,318	Succinate dehydrogenase, iron-sulfur protein
W6QSV5	BN5_1416	0,036	3,217	Dihydroorotate dehydrogenase (quinone)
W6QXM5	BN5_3063	0,008	3,183	Oxidoreductase FAD/NAD(P)-binding subunit
W6R4K8	BN5_2718	0,034	3,152	4-hydroxy-tetrahydrodipicolinate synthase
W6RDZ3	BN5_1509	0,016	3,104	Arc
W6R3G9	BN5_2367	0,021	3,060	Extracellular solute-binding protein
W6QWY7	BN5_2815	0,047	3,041	2-dehydro-3-deoxyphosphooctonate aldolase
W6R638	BN5_3265	0,008	3,027	Co-chaperone protein HscB homolog
W6REY3	BN5_1853	0,008	2,986	Isocitrate lyase
W6RE08	BN5_1524	0,021	2,906	Fumarate hydratase class II
W6RC63	BN5_0860	0,008	2,858	Probable malate:quinone oxidoreductase
W6RHT1	BN5_2814	0,049	2,789	Enolase
W6QW01	BN5_1577	0,042	2,768	Molybdenum cofactor guanylyltransferase
W6RL00	BN5_4017	0,040	2,695	Dihydroxy-acid dehydratase
W6QU70	BN5_1433	0,018	2,663	Uncharacterized protein
W6QU53	BN5_1854	0,018	2,655	Uncharacterized protein
W6R3B3	BN5_2295	0,007	2,622	MarR family transcriptional regulator
W6R9C0	BN5_4452	0,012	2,602	Alkyl hydroperoxide reductase AhpD
W6QSJ5	BN5_0349	0,049	2,510	Fructose-bisphosphate aldolase, class II

W6R2R6	BN5_4453	0,015	2,509	Uncharacterized protein
W6QWB1	BN5_1672	0,047	2,479	5-methylthioadenosine/S-adenosylhomocysteine deaminase
W6QXN7	BN5_3079	0,001	2,466	OmpA domain-containing protein
W6R2N8	BN5_3956	0,040	2,450	GTP-binding protein TypA/BipA
W6R242	BN5_4228	0,003	2,445	Uncharacterized protein
W6R2Y2	BN5_2160	0,009	2,431	Arylesterase
W6QPP2	BN5_0301	0,006	2,378	Beta-ketoacyl synthase
W6RGP7	BN5_2510	0,008	2,364	RND family efflux transporter MFP subunit
H9N5D9	BN5_1636	0,009	2,361	Uncharacterized protein
W6QWH8	BN5_1757	0,004	2,333	Aconitate hydratase B
W6QXM1	BN5_0287	0,019	2,288	Phosphoenolpyruvate carboxykinase [ATP]
W6QXL3	BN5_0277	0,030	2,273	Phenylacetic acid degradation-related protein
W6QV55	BN5_2179	0,023	2,273	Succinate dehydrogenase flavoprotein subunit
W6RCA6	BN5_0915	0,008	2,214	Carbamoyl-phosphate synthase small chain
W6RI94	BN5_2964	0,029	2,182	Isochorismatase hydrolase
W6QSF0	BN5_0823	0,003	2,139	Uncharacterized protein
W6R3P5	BN5_4264	0,020	2,023	PpkA-related protein
W6QTP6	BN5_0719	0,034	2,007	Extracellular solute-binding protein
W6R3H6	BN5_4204	0,031	2,004	Heme-binding protein A

[1]Protein accesion number from UniProt, [2]gene accession number from GeneBank (Luque-Almagro *et al.* 2013); [3]Fold Change. Only proteins with a *p*-value ≤ 0.05 and a fold change ≥ 2 were considered.

Table S3. Comparative analysis of *nitA*⁻ and *nitC*⁻ mutants. Induced proteins in *nitA*⁻ mutant.

Protein accession number[1]	Gene accession number[2]	*p*-value	F.C.[3]	Description
W6QU73	BN5_1879	0,001	46,556	Putative Anthranilate phosphoribosyltransferase
W6QXL4	BN5_2662	0,000	45,095	Flagellin
W6REH9	BN5_1658	0,003	44,734	Helix-hairpin-helix repeat-containing competence protein ComEA
W6R110	BN5_1506	0,001	34,471	Uncharacterized protein
W6QWK6	BN5_1792	0,012	33,796	3-oxoacyl-(Acyl-carrier-protein) synthase I
W6QXF1	BN5_2980	0,009	24,877	OmpA/MotB domain-containing protein
W6QPC7	BN5_0176	0,000	23,960	Mg chelatase, subunit ChlI
W6R0A3	BN5_3590	0,003	23,322	Fatty-acyl-CoA synthase
W6QNX3	BN5_0029	0,015	21,088	DNA protecting protein DprA
W6QTC3	BN5_0616	0,003	16,206	Alpha-2-macroglobulin domain-containing protein
W6R3F4	BN5_2347	0,028	15,130	Cytochrome c550
W6RK11	BN5_3592	0,003	14,879	Acyl-CoA dehydrogenase family protein
W6QXP8	BN5_3089	0,005	12,817	Aspartyl-tRNA synthetase
W6QXI2	BN5_0237	0,011	12,629	Membrane-fusion protein
W6QYF6	BN5_2952	0,010	10,362	Outer membrane porin
W6R4D5	BN5_2661	0,002	9,600	Protein flaG
W6RGZ5	BN5_2624	0,000	9,067	ParA family protein
W6QZ68	BN5_0862	0,033	8,938	Uncharacterized protein
W6QY39	BN5_2349	0,024	8,884	Pentapeptide repeat-containing protein
W6R3S5	BN5_4294	0,000	8,201	Uncharacterized protein
W6QWU6	BN5_0015	0,012	7,591	Glycine--tRNA ligase beta subunit
W6R8B1	BN5_4106	0,000	7,271	Secretion protein HlyD family protein
W6QTW8	BN5_1759	0,009	7,206	Universal stress protein E homolog
W6R8V0	BN5_4267	0,026	6,983	Putative virulence effector protein
W6RI31	BN5_2889	0,050	6,727	Uncharacterized protein
W6R3W1	BN5_2507	0,015	6,721	Uncharacterized protein
W6QYR0	BN5_0639	0,003	6,230	Uncharacterized protein
W6QR33	BN5_0771	0,015	5,969	CRISPR-associated Cas5e family protein
W6RH20	BN5_2649	0,010	5,934	Flagellar assembly protein H
W6QY43	BN5_2354	0,021	5,761	ABC transporter periplasmic protein
W6R686	BN5_3331	0,001	5,722	Arginine deiminase
W6R848	BN5_4039	0,023	5,513	UPF0339 protein in ptx operon 5'region
W6QZ01	BN5_0772	0,005	5,493	CRISPR-associated Cse3 family protein
W6RDL1	BN5_1358	0,046	5,158	Probable malate:quinone oxidoreductase
W6QWS2	BN5_2737	0,003	4,693	Aminopeptidase N
W6QWH4	BN5_2670	0,020	4,625	Flagellar P-ring protein
W6R217	BN5_1865	0,007	4,538	Cold shock-like protein cspG
W6R1Z2	BN5_3706	0,020	4,444	50S ribosomal protein L1
W6QY19	BN5_0447	0,046	4,124	Putative Universal stress protein E
W6QXH7	BN5_2627	0,002	4,085	Chemotaxis response regulator protein-glutamate methylesterase
W6QUY3	BN5_1671	0,026	3,294	Ubiquinone biosynthesis O-methyltransferase
W6QS57	BN5_0728	0,029	3,268	Glutamyl-tRNA(Gln) amidotransferase subunit A
W6R4U4	BN5_2831	0,047	3,262	Ribosome-recycling factor
W6R5F1	BN5_3049	0,027	3,172	Glyceraldehyde-3-phosphate dehydrogenase
W6RKL0	BN5_3786	0,008	2,799	RNA polymerase sigma factor RpoD
W6QSI2	BN5_0853	0,007	2,774	3-ketoacyl-(Acyl-carrier-protein) reductase
W6R2E7	BN5_3881	0,004	2,753	Putative c repressor
W6R012	BN5_3500	0,027	2,732	Anti-sigma-factor antagonist
W6R194	BN5_3950	0,044	2,725	Uncharacterized protein
W6QUL0	BN5_1576	0,012	2,511	Putative lipoprotein ygdI
W6RG82	BN5_2313	0,035	2,466	CopG family transcriptional regulator
W6QXQ8	BN5_2682	0,010	2,400	Putative flagella synthesis protein FlgN
W6R5A3	BN5_3001	0,039	2,336	3-hydroxyisobutyrate dehydrogenase
W6RE51	BN5_1572	0,022	2,130	Uncharacterized protein
W6RHV8	BN5_2834	0,008	2,116	30S ribosomal protein S2
W6RHN5	BN5_2779	0,036	2,077	Nitrate reductase

Protein accesion number from UniProt, [2]Gene accession number from GeneBank Luque-Almagro *et al.,* 2013); [3]Fold Change. Only proteins with a *p*-value ≤ 0.05 and a fold change ≥ 2 were considered.